



University of
Stavanger

FACULTY OF SCIENCE AND TECHNOLOGY

MASTER'S THESIS

Study programme/specialisation:

Engineering Structures and
Materials/Mechanical Systems

Spring/ ~~Autumn~~ semester, 2020.

Open / ~~Confidential~~

Author: Abdullahi Sagir

Programme coordinator: Dimitrios Pavlou

Supervisor(s):

Ove Kjetil Mikkelsen – Main supervisor

Mostafa Ahmed Atteya – Co-supervisor

Title of master's thesis:

Stress Analysis of Simple Tubular joints – Loaded chord members.

Credits:

30 ECTS

Keywords:

Abaqus/CAE

Finite Element Analysis

Hot spot stress

Stress concentration factors

Fatigue life evaluation

Loaded chord members

Number of pages:

+ supplemental material/other:

Stavanger, 29th June 2020

date/year

Abstract

This thesis covered the subject of stress analysis in simple tubular joints, with a focus on tubular joints with loaded chord members. The type of loading investigated is even though quite common, not very much investigated. This is referring to local loads on joints that may come from minor sources such as installation of mechanical clamps around the local area of joints. This type of loading can have an effect on the overall fatigue performance of the joints and by extension the structures in which they are present.

Finite element analysis with shell elements was used a tool to investigate stress concentration in such joints. Chord loading was defined as a distributed circumferential vertical load at defined distance away from chord crown positions. Stress concentration factors and where relevant, fatigue life(s) were determined using both FEA and parametric equations from DNV-RP-C203. For some of the joints, FEA results were directly compared to results from standard, while for other joints, results from standard were only used as a reference point for FEA results. For the tubular joints with loaded chord members, focus was mainly on finding stress concentration factors on the chord side of the joint intersection. i.e the crown and saddle positions of the chord.

Acknowledgement

This thesis was written at the Faculty of science and technology, University of Stavanger. This is in partial fulfilment for a Master of science degree in Mechanical and structural engineering and material science. I wish to express my gratitude to all those that assisted me one way or the other towards making the journey a success.

Special thanks to my main supervisor in the person of Ove Mikkelsen, and co-supervisor Mostafa Atteya for their support and guidance, as well as academic competence. Your efforts are well appreciated and duly acknowledged.

Table of Contents

Summary	i
Preface	ii
Table of Contents	v
List of Tables	vi
List of Figures	viii
Abbreviations	ix
1 Introduction	1
1.1 Background	1
1.2 Objective	3
1.3 Limitations	4
1.4 Organization of thesis	4
1.4.1 Chapter 1	4
1.4.2 Chapter 2	4
1.4.3 Chapter 3	4
1.4.4 Chapter 4	5
1.4.5 Chapter 5	5
2 Theoretical background	6
2.1 Introduction	6
2.2 Classification of tubular joints	7
2.3 Geometric parameters for tubular joints	10
2.4 Stress analysis of tubular joints	10
2.4.1 Nominal stress	11
2.4.2 Geometric stress	12
2.4.3 Notch stress	12

2.4.4	Hot spot stress	13
2.5	Stress concentration factors	13
2.5.1	Experimental method	14
2.5.2	Simple joints SCF equations	15
2.5.3	Finite element method FEM	17
2.6	Fatigue life evaluation	19
2.6.1	The S-N Approach	20
3	Stress analysis of simple tubular joints	22
3.1	Stress concentration factors by design code	22
3.1.1	Stress concentration factor SCF	22
3.1.2	Fatigue life estimation	24
3.2	Stress concentration factors by Abaqus CAE	25
3.2.1	Part module	26
3.2.2	Assembly module	26
3.2.3	Step module	27
3.2.4	Interaction module	28
3.2.5	Load module - Load and boundary condition	28
3.2.6	Mesh module	29
3.2.7	Derivation of hot spot stresses	31
3.2.8	Mesh convergence study	34
3.2.9	Stress concentration factors SCF	36
3.2.10	Fatigue life estimation	37
3.3	Comparison of FEA and DNV results	38
4	Stress analysis of simple tubular joints with loaded chord members	40
4.1	Introduction	40
4.2	Effect of chord stresses on SCFs	40
4.3	Finite element modelling	41
4.3.1	Load Module - Load and boundary condition	41
4.3.2	Checks for FEM models	42
4.3.3	Averaging of results in Abaqus	43
4.4	Stress concentration factors	44
4.5	Model I	44
4.5.1	Results and observations	45
4.6	Model II	48
4.6.1	Results and observations	48
4.7	Model III	50
4.7.1	Results and observations	50
4.8	Model IV	53
4.8.1	Results and observations	54

5 Conclusion	57
5.1 Discussion	57
5.1.1 Stress concentration using Eftymiou equations	57
5.1.2 Stress concentration using FEA	58
5.1.3 Factors influencing the effect of chord loading	59
5.2 Conclusion	60
5.3 Further work	61
Bibliography	61
Appendix	64

List of Tables

2.1	Validity range for Kuang equations	15
2.2	Validity range for Wordsworth/Smedley equations	16
2.3	Validity range for Efthymiou/Durkin equations	16
3.1	Geometric parameters for the joint under consideration.	23
3.2	Stress concentration factors using DNV-RP-C203.	23
3.3	S-N curve for tubular joints in air DNV-RP-C203.	25
3.4	Fatigue life estimation using DNV-RP-C203.	25
3.5	Definition of joint parameters.	26
3.6	Material properties.	26
3.7	Magnitude and direction of loads applied under different loading modes.	29
3.8	Definition of points for readout of stresses and weld toe at different locations.	35
3.9	Details for defining Abaqus/CAE model.	37
3.10	Stress concentration factors using Abaqus/CAE.	37
3.11	Fatigue life estimation using Abaqus/CAE.	38
3.12	Stress concentration factors for T-joint using Abaqus and Efthymiou equations.	39
3.13	Comparison between estimated fatigue life(s)	39
4.1	Summary of Model I	45
4.2	SCF from FEA T-joint with loaded chord member.	46
4.3	Definition of joint geometry.	48
4.4	Summary of Model II	48
4.5	SCF from FEA T-joint with loaded chord member.	49
4.6	Definition of joint geometry.	51
4.7	Summary of Model III	51
4.8	SCF from FEA T-joint with loaded chord member.	52
4.9	Definition of joint geometry.	54
4.10	Summary of Model IV	54
4.11	SCF from FEA Y-joint with loaded chord member.	56

List of Figures

1.1	Stress analysis of tubular joints [25].	2
1.2	Tubular joint with loaded chord member.	3
2.1	Example of a tubular joint in an offshore structure along side its geometric notation [2].	6
2.2	Geometrical definitions of tubular joints. [4]	7
2.3	Joint classification according to force transfer [9].	8
2.4	Brace-chord classification according to force transfer [9].	9
2.5	Determining the components of joint action in braces [24].	9
2.6	Basic tubular joints load cases [25].	11
2.7	Nominal stress distribution in Chord and brace sides [14].	11
2.8	Geometric stress distribution in Chord and brace sides [14].	12
2.9	Notch stress distribution in Chord and brace sides [14].	12
2.10	Hot spot stress distribution in Chord and brace sides [14].	13
2.11	stress concentration in an axially loaded T-joint [25].	14
2.12	Tubular T-joint test. [8]	15
2.13	Typical S-N curves [13].	20
3.1	T or Y-joint [9].	23
3.2	S-N curve for tubular joints in air and in sea water under cathodic protection. [7]	24
3.3	Instance of T-joint showing partitions.	27
3.4	Defining analysis step for axial loading.	27
3.5	Constraints for application of load and boundary conditions.	28
3.6	Definition of axial loading.	29
3.7	Definition of boundary conditions.	29
3.8	Seeding of part instance for mesh generation.	30
3.9	Element type window.	31
3.10	Mesh control window.	31
3.11	Points for read-out of stress for calculation of HSS [7].	32

3.12	Welding profiles at both saddle and crown positions for determination of a and b locations. [23].	33
3.13	Example of derivation of hot spot stress. [7].	33
3.14	4 node plane element in physical space (left) and the same element mapped into $\xi \eta$ space (right). [19].	34
3.15	Sampling points for integration using Gauss rule of order 2. [19].	34
3.16	Illustration of points for readout of stresses at the chord saddle position.	35
3.17	Derivation of hot spot stress.	36
3.18	Estimated SCFs with respect to number of elements for S4R and S8R elements compared to the SCF from Efthymiou equations.	37
4.1	Illustration of application of chord load.	42
4.2	Boundary condition of model of left and right sides of chord member.	42
4.3	Contour plots for Mises stress using different averaging options.	43
4.4	Illustration of partition lines for application of chord load.	45
4.5	Contour plots for Mises stress showing averaged and unaveraged results.	46
4.6	Extrapolation of stresses at point a and b to the hot spot for the 1/8 loading case.	46
4.7	Extrapolation of stresses at point a and b to the hot spot for the 1/4 loading case.	47
4.8	Extrapolation of stresses at point a and b to the hot spot for the 1/2 loading case.	47
4.9	Contour plots for Mises stress showing averaged and unaveraged results.	49
4.10	Extrapolation of stresses at point a and b to the hot spot for the 1/8 loading case.	50
4.11	Extrapolation of stresses at point a and b to the hot spot for the 1/4 loading case.	50
4.12	Extrapolation of stresses at point a and b to the hot spot for the 1/2 loading case.	51
4.13	Contour plots for Mises stress showing averaged and unaveraged results.	52
4.14	Extrapolation of stresses at point a and b to the hot spot for the 1/8 loading case.	53
4.15	Extrapolation of stresses at point a and b to the hot spot for the 1/4 loading case.	53
4.16	Extrapolation of stresses at point a and b to the hot spot for the 1/2 loading case.	54
4.17	Illustration of partition lines for application of chord load for the Y-joint.	55
4.18	Contour plots for Mises stress showing averaged and unaveraged results.	55
4.19	Extrapolation of stresses at point a and b to the hot spot for the 1/4 loading case.	56
4.20	Extrapolation of stresses at point a and b to the hot spot for the 1/2 loading case.	56

Abbreviations

CAE	=	Complete Abaqus environment
DNV	=	Det Norsk Veritas
ABS	=	American Bureau of Shipping
CHS	=	Cylindrical hollow section
RHS	=	Rectangular hollow section
SHS	=	Square hollow section
SCF	=	Stress concentration factor
FEM	=	Finite element method
FEA	=	Finite element analysis
DT	=	Double T
DK	=	Double K
DY	=	Double Y
IPB	=	In-plane bending
OPB	=	Out-of-plane bending
AC	=	Axial compression
HSS	=	Hot spot stress
MPC	=	Multi point constraint
CS	=	Chord saddle
CC	=	Chord crown
BS	=	Brace saddle
BC	=	Brace crown

Introduction

1.1 Background

Tubular structures are widely used in offshore installations, these structures are mainly constructed as three-dimensional frames comprising tubular members as structural elements. In offshore platforms, cylindrical hollow sections (CHS) are typically used. While rectangular hollow sections (RHS) and square hollow sections (SHS) are most commonly used in trusses and high rise buildings. Tubular sections have inherent properties that allow them to minimize hydrodynamic forces and possess high torsional rigidity. They are also reported to give the best compromise in satisfying the requirements of low drag coefficient, high buoyancy and high strength-to-weight ratio [22]. The space inside the hollow section can also be used for transport or to obtain additional strength by the use of internal support. This allows them to deliver excellent structural performance in addition to an attractive architectural appearance. Because of these advantages, tubular structures are used in various structural applications.

The most common offshore application is in the design of jacket structures used for drilling and production of oil and gas. Some of these structures are installed in very hostile environments which exposes them to several types of cyclic environmental and operational loads including, wind, waves, currents, earthquakes etc. In addition, gravity loads also exist, gravity loads arise from dead weight of structure and facilities that are either permanent or temporarily installed in the structures. An example includes structural dead loads, facility dead loads, fluid loads, live loads etc. The environmental loads play a major role in governing the design of offshore structures. The loads mentioned above are more global both in their application and in the effects they cause on the overall fatigue performance of the structure, However, there is a class of loading which is common but not quite investigated. This is referring to local loads on joints that may come from minor sources such as the installation of sacrificial anodes or application of mechanical clamps around the local areas of joints. Figure 1.2 gives an illustration. Overall, These loads cause time varying stresses which can lead to fatigue damage in critical joints in the structures. According to [3], Fatigue cracking has been regarded as the main cause of damage to North

sea steel structures. Therefore, in order to ensure structural integrity, joint design for offshore structures is controlled by fatigue performance in addition to static strength. It is for the same purpose that exists dedicated standards providing guidelines for the overall and detail design methodology for fatigue in offshore structures. A typical example is the DNV-RP-C203 which is the main standard used in this project.

In the fatigue design of offshore structures, both the structural members (elements), and joints must be designed to sustain the ultimate design load, (e.g. the 100-year design condition), as well as the long term cyclic stresses due to long term action. The design process includes both a global and local analysis of the structure. The global analysis determines the sectional forces and the nominal member stresses in the various elements of the structure. The results obtained from the global analysis establish the boundary conditions for the local analyses of the structural joints. The local analyses of simple tubular joints will be the focus of this project. This problem boils down to a detailed examination of the stresses in simple tubular connections with known geometry and boundary conditions. This will mainly involve the determination of stress concentration factors as well as fatigue life of joints using established principles. These exercises allow for more effective joint designs by allowing engineers to have a good understanding of structural behaviour, and of the stress systems in operation. Figure 1.1 below illustrates how tubular joints are applied in offshore structures as well as a breakdown of the stages involved in study of the stress systems present in such structures.

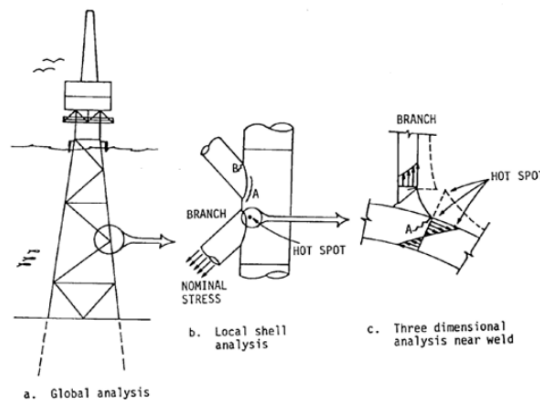


Figure 1.1: Stress analysis of tubular joints [25].

Generally, it is impractical to inspect all joints and members in offshore structures due to high cost of inspection, thus inspections are only carried out on selected critical joints. For some of these joints, the stress concentration can produce a maximum stress at the intersection as high as 20 times the nominal stress acting in the members [17]. As a result an accurate prediction of stress concentration is of utmost importance in the design of tubular joints.



Figure 1.2: Tubular joint with loaded chord member.

1.2 Objective

The objective of this thesis is to carry out stress analysis of simple tubular joints. This objective is considered under two main categories, The first category involves the study of stress concentration in simple tubular joints under the three basic loading conditions, while the second category is the assessment of tubular joints with loaded chord members. The competence built from the first category will form the basis for carrying out the second objective. Stress concentration in welded joints of tubular structures is an important consideration for fatigue design of offshore structures. The finite element method provides a convenient, less time consuming and cost effective means of estimating the fatigue life for tubular joints. Starting with the most basic type of tubular joint, the T-joint, this project aims to verify both the stress concentration factors (SCF) and fatigue life(s) calculated using design code against values obtained using the finite element analysis software Abaqus/CAE. DNV-RP-C203 has covered extensively the procedures for the determination of stress concentration factors using parametric equations, as well as fatigue life estimation for most joints in common use. Fatigue life(s) will be estimated using the S-N approach. The study will cover tubular joints under axial loading, in-plane bending and out-of-plane bending.

Generally only one member (Chord or brace) is loaded at a time while evaluating SCFs, the first objective of this thesis is to load the brace member with the three basic loading cases mentioned previously, and then later modify the scenario by including in addition to the load on the brace, a vertical circumferential load on the chord, acting in a direction perpendicular to the chord axis. A joint under this combination of loading will henceforth be referred to in this report, as a tubular joint with loaded chord member. Additional hot spot stresses are said to be generated if the chord or other members are also loaded along with the brace member in a joint. The effects of this additional hot spot stress on the stress concentration factors at different locations around the joint intersection will be investigated.

1.3 Limitations

As mentioned previously, this investigation aims to assess fatigue performance of joints using parametric equations from DNV standard, DNV-RP-C203 and compare against results obtained using finite element method (FEM). With FEM, any arbitrary case can be investigated using an adequate definition of the model, including the case that this investigation aims to study. However the standard to be used for comparison only covers certain cases/instances of the stress concentration problem in tubular joints. The stress analysis of tubular joints with loaded chord members has not been covered by DNV-RP-C203 which will be considered as a source of reference for comparison. There is also very limited resources available in the literature regarding tubular joints with loaded chord members, this is considered as a source of limitation for this investigation.

1.4 Organization of thesis

This report is organized into five chapters as follows;

1.4.1 Chapter 1

This chapter gives an introduction to the problem, a brief overview for the applications of tubular joints in offshore structures, leading to the motivation behind the study. It also outlines the objectives as well as the limitations of the study.

1.4.2 Chapter 2

This chapter covers the fundamental concepts that form the basis for fatigue analysis of tubular joints. This includes classification of joints, stress concentration and fatigue life evaluation of tubular joints.

1.4.3 Chapter 3

This chapter covers the ground work upon which the competence to study tubular joints with loaded chord members was built. This involved the determination of stress concentration factors and fatigue life(s) for a simple T-joint using both FEA and DNV-RP-C203. This was performed under the three basic loading modes in tubular joints. For the FEA, a mesh convergence study was carried out. Results from FEA and DNV-RP-C203 were compared.

1.4.4 Chapter 4

This chapter covers the main work for investigating tubular joints with loaded chord members. A total of four joints were investigated under axial loading on the brace as well as a distributed vertical circumferential load on the chord. Focus was mainly on finding the effect of chord loading on the stresses that arise in the chord members of the joints. SCFs were determined from FEA and compared to values obtained using the Efthymiou equations.

1.4.5 Chapter 5

This chapter covers a discussion of the results as well as a conclusion of the study.

Theoretical background

2.1 Introduction

This chapter covers a discussion of the fundamental concepts that provide the basis for performing fatigue analysis of tubular joints. This includes a brief general classification of tubular joints based on geometry as well as balance of forces, definition of the geometric parameters used to define tubular joints, a discussion of the main stress systems common in tubular joint configurations, simple joints stress concentration factor equations, as well as the fundamental principles used in fatigue life evaluation. This chapter also comprises a summary of the finite element method (FEM), the basic theories that allow the investigation of stress concentration using FEM. Figure 2.1 below gives an illustration of the application of tubular joints in offshore jacket structures alongside the geometric notations used to classify these joints.

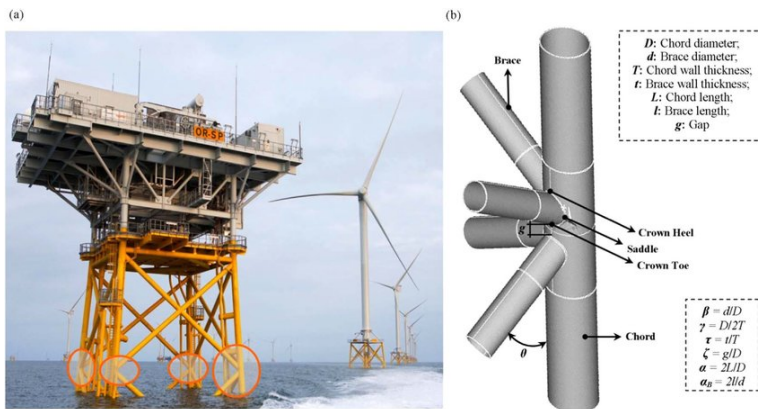


Figure 2.1: Example of a tubular joint in an offshore structure along side its geometric notation [2]

2.2 Classification of tubular joints

Jacket structures are constructed from diverse types of joints, the configurations of which are normally chosen to provide the best horizontal and torsional resistance to the particular environmental forces under consideration. The number, size and orientation of the members meeting at a joint vary significantly depending on the size and configuration of the structures in which they are used. Generally, joints are classified into four main categories based on fabrication;

1. Simple welded joints
2. Complex welded joints
3. Cast steel joints
4. Composite joints

Each joint type possess different design and fabrication challenges and each require different treatment. For the purpose of this project, we focus on the "simple joint" category. A joint is considered to belong to this category only when it is formed by welding two or more tubular members in a single plane without the overlap of brace members and without use of gussets, diaphragms, stiffeners, or grout. The circular hollow sections coming together to form the joint are classified into chord and brace(s) in such manner that; For a two member joint, the chord member is the one with the larger diameter and the other is treated as a brace. In the case of members having equal diameters, the one with the thicker wall is considered as the chord member. And in case the of members with equal diameter and thickness, the most horizontal member is taken as the chord member. On the other hand, the term complex welded joints is used for joints with uni-planar or multi-planar overlapping brace members, joints with internal and/or external stiffeners or diaphragms and other less readily categorised joints.

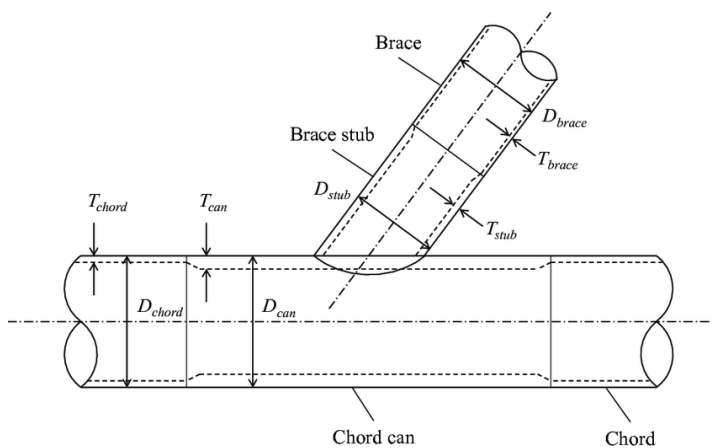


Figure 2.2: Geometrical definitions of tubular joints. [4]

It is common for simple tubular joint to contain a short length of thicker walled tube, sometimes of higher strength material, in the connection area. Or as illustrated in Figure 2.2, designed to have thicker-walled brace tubular sections close to the joint. This is in order to prevent excessively high local stresses and to provide adequate static strength.

There is a more design inclined classification of tubular joints which requires proper consideration of the applied loads and joint configurations, this method is based on force transfer in the joint rather than its physical appearance. The basic types of joint configurations in this method are T, X and K or N joints.

a). A joint where the normal component of the brace member force is balanced by beam shear (and bending) in the chord member, is classified as a T joint when the brace is perpendicular to the chord, if the brace meets the chord at an acute angle, the joint is classified Y.

b). When the normal component of a brace member force is essentially balanced (within 20 percent) by the normal force component of another brace member (or members), on the same side of the joint, the joint is classified as a K joint [24] . For this type of joints, two braces come together on one side of the chord so that the center line of each brace forms an acute angle with the axis of the chord. An N joint is a special type of K joint.

c).When the normal force component is transmitted through the chord member and is balanced by a brace member (or members) on the opposite side of the chord, the joint is classified as an X joint. This configuration is also considered as a combination of single Y joints.

d).Other configurations with members on opposite sides of the chord are possible, these are known as double joints. Their single counterparts are formed by combining mirror images of the corresponding single joint. There are three basic configurations in this category; DT, DY and DK.

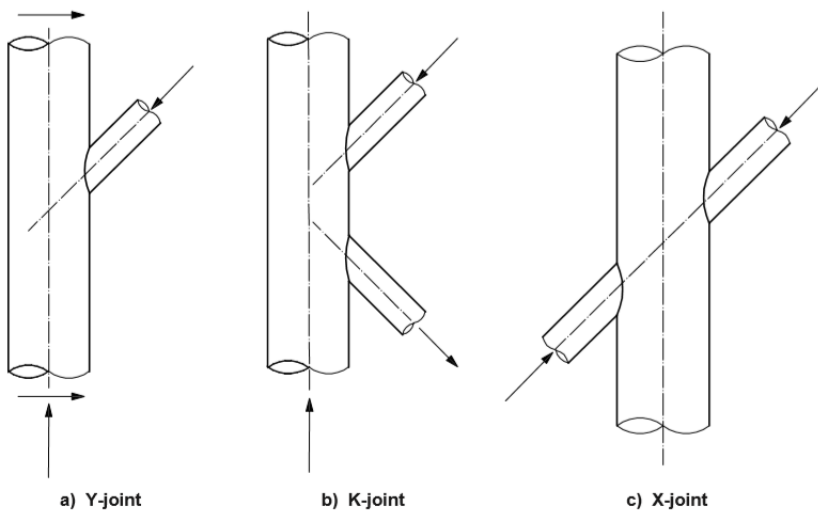


Figure 2.3: Joint classification according to force transfer [9] .

A joint is classified as a combination of Y-,K- and X-joints when the behaviour of the braces contains elements of the behaviour of more than one type. This classification applies to the combination of an individual brace with the chord, rather than to the whole joint, on the basis of the axial force pattern for each load case. For example, If the brace-chord combination carries part of the axial brace force as a K-joint, and part as a Y-joint or X-joint, it shall be classified as a proportion of each relevant type, e.g. 50 percent as a K-joint and 50 percent as an X-joint. Figure 2.4 gives an illustration of such, whereby braces are either fully of a particular type or classified as a mixture of classes.

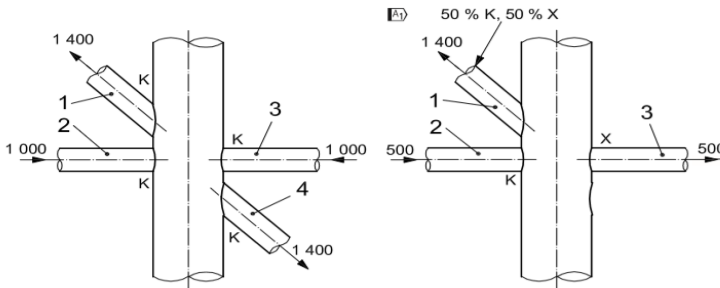


Figure 2.4: Brace-chord classification according to force transfer [9] .

When performing an analysis of a joint, it is critical that an appropriate classification of each brace-chord pair is carried out. Figure 2.5 illustrates such example where the two braces forming the joint can be checked in order to appropriately classify them. Applying the equilibrium condition about the joint intersection and utilizing a brace-chord angle of 38.7 degrees, the lower part of the figure shows a balance of forces illustrating the combination of joint actions present in each of the braces. As can be seen, the leftmost brace is made up of both K- and X-joint actions in approximately 60 and 40 percentages respectively, while the rightmost brace is made of a 100 percentage K-joint action.

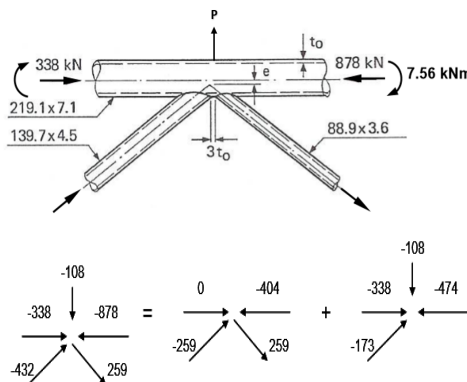


Figure 2.5: Determining the components of joint action in braces [24] .

2.3 Geometric parameters for tubular joints

The geometric parameters used to define tubular joints vary according to the type of the joint. However, some of these parameters are fundamental and are shared by most joint types. They are non dimensional parameters that describe joint properties such a chord stiffness, wall thickness ratio, etc. For example, the chord stiffness parameter (γ) describing the chord radial stiffness is a very important parameter in many formulations of stress concentration. Parameters are calculated from geometric dimensions of the members that make up the joint. In the design of tubular joints, each brace is considered separately in relation to the chord in order to calculate a geometric parameter. A more symbolic description of these parameters as provided in DNV-RP-C203 is shown in the appendix of this report, but generally, the following non dimensional parameters are used.

- Chord length parameter α : This is defined as the ratio of chord length L , to chord radius $D/2$. It gives an indication of chord beam characteristics.
- Chord thinness ratio γ : This is defined as the ratio of chord radius to chord wall thickness. It gives an indication of thickness and radial stiffness of the chord.
- Diameter ratio β : This is defined as the ratio of the brace diameter to chord diameter. It describes the compactness of the joint.
- Wall thickness ratio τ : This is defined as the ratio of the brace to chord wall thickness (t/T). It is a measure of the likelihood of chord wall failure before brace cross section fracture.
- Gap parameter ς : This is defined as the ratio of the gap between braces to chord diameter. It describes the proximity of other brace members to the subject brace member for joints with more than one brace.

2.4 Stress analysis of tubular joints

The stress analysis problem of tubular joints in offshore structures has been extensively studied over the past several years, both experimentally and analytically. The main purpose of conducting stress analyses of tubular joints is to obtain information on the Hot spot stress (HSS) and by extension, the stress concentrations around the intersections for fatigue assessment [12]. From local linear stress analysis, studies have shown that stresses concentrations mainly occur near the welded intersections, thus, areas of stress concentration are practically always found in the joints and not in the members themselves. The mechanism works as such, forces subjected to the structure itself transition into stresses observed around joints, the variation of force transition is dependent on the section property of the arbitrary joint member, as well as the load combination of the three basic load modes. Offshore structures are exposed to multi-axial loading, i.e. a combination of axial forces, in-plane bending (IPB) and out-of-plane bending (OPB) moments, which are illustrated separately by Figure 2.6 below. The underlying stress systems present are discussed in sections 2.4.1 - 2.4.4 below;

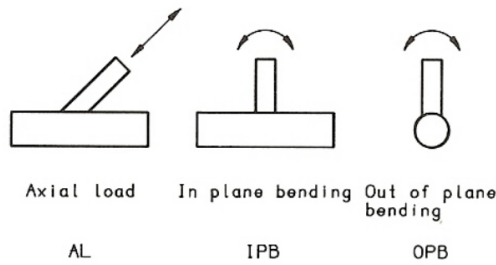


Figure 2.6: Basic tubular joints load cases [25].

2.4.1 Nominal stress

Otherwise known as the engineering stress, the nominal stress is the basic structural response of a joint to applied loads. This form of stress arises from the framing action of the jacket structure under applied external loads. It is calculated by the global analysis of the structure using a relevant software package e.g. SAP2000, or by the use of the simple beam theory. The simple beam theory expresses the stress as a function of either an axial force only, a moment force only, or a combination of both. The equation below is an expression of the nominal stress according to the simple beam theory, where N is the applied axial compressive load, A is the cross sectional area, M is the applied bending moment, y is the position of the extreme fibre and I is the moment of inertia.

$$\sigma_{nom} = \frac{N}{A} \pm \frac{My}{I}$$

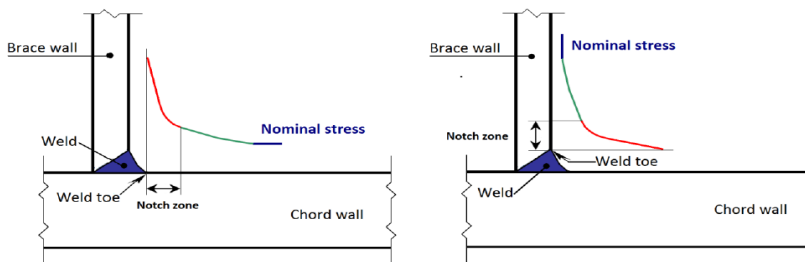


Figure 2.7: Nominal stress distribution in Chord and brace sides [14].

2.4.2 Geometric stress

Geometric stress, also known as the structural hot stress is a stress field that arises due to difference in the load response exhibited by the brace and chord under a given loading condition. For example, when there is a difference in deformation between the brace and the chord, the tube wall bends in order to maintain compatibility in the deformation of the chord and brace around the intersection. This stress includes nominal stresses and stresses from structural discontinuities but do not include stresses due to the presence of welds. It is commonly used to determine the fatigue life of tubular joints.

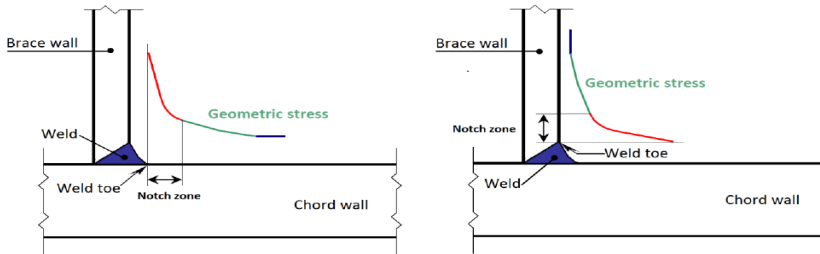


Figure 2.8: Geometric stress distribution in Chord and brace sides [14] .

2.4.3 Notch stress

The notch stresses also known as the local stresses are the result of geometric discontinuity of the tubular walls at the weld toes where an abrupt change of section occurs. This stress include the notch effect occurring along the notch zone [22] . They are known as local stresses because they do not propagate far through the wall thickness which results in a local region where stresses vary rapidly in three dimensions. Local stresses are a function of the weld geometry and size, and thus it is mainly dependent on the quality of welding and workmanship. It is also reported to be quite difficult to incorporate their effect into formulation of stress concentration.

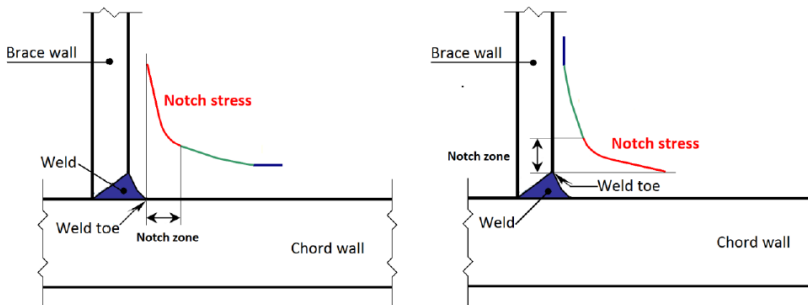


Figure 2.9: Notch stress distribution in Chord and brace sides [14] .

2.4.4 Hot spot stress

This refers to the maximum stress caused by applied external loads on the joint. The hotspot stress occurs in what is known as the 'hot-spot', which is a point on the structure where a fatigue crack may initiate under a cyclic load, due to the combined effect of structural stress fluctuation, as well as the weld geometry or a notch. In other words, the hot-spot stress is the surface value of the structural stress at hot-spots. For the types of joints studied in this project, the hot-spots are located in the intersection between the brace and the chord for non welded tubular joints, and at the weld toes for welded joints. The definition of this stress field sets the foundation for the application of the Hot-spot stress method for fatigue life analysis of tubular joints. In order to determine the Hot-spot stress (HSS) using finite element analysis (FEA), the stresses at two locations away from the weld toe are discovered, these stresses are then linearly extrapolated to the weld toe in order to determine the HSS. While according to the design code, DNV-RP-C203, the HSS is determined based on nominal stress and stress concentration factors achieved using parametric equations. Both approaches are employed in this project.

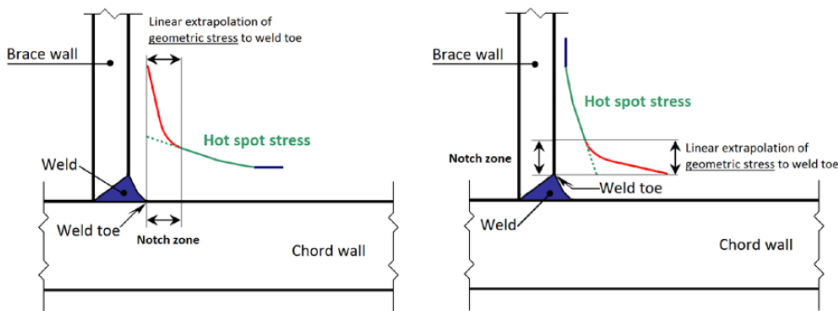


Figure 2.10: Hot spot stress distribution in Chord and brace sides [14].

2.5 Stress concentration factors

The stress concentration factor (SCF) in tubular joints is defined as a relationship between the stress recorded at a local area of extra-high stress and the nominal brace stress. Investigation has shown that there are two areas where the most stress rising effect occur, one is the weld toe at the brace side, and the other at the weld toe at the chord side. These points are known as the hot spots. As mentioned previously, local stresses at these points are several times higher than the nominal brace stress, thus the load transferred to the weld is not even. This is a result of the difference in the relative stiffness of the chord and brace. For example, in an axially loaded T-joint as in Figure 2.11, the thin chord wall is inefficient at supporting normal loads as compared to in-plane loads. As a result, large bending stress occur due to ovalisation of the chord [25]. The SCF definition lays an important foundation for the fatigue assessment of tubular joints. Stress concentration factors are determined using finite element analysis, experimental methods, or empirical parametric

equations determined from any of the two previous methods. These methods are discussed in the upcoming sections.

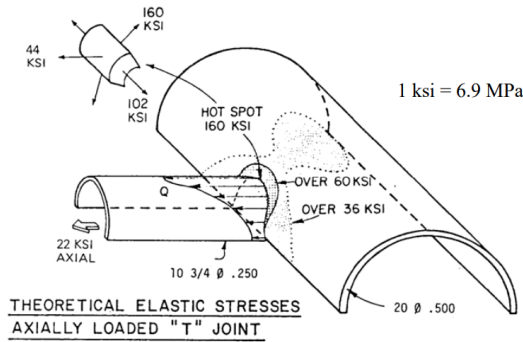


Figure 2.11: stress concentration in an axially loaded T-joint [25] .

2.5.1 Experimental method

The main purpose of laboratory tests is design substantiation through physical model testing. Physical model testing is the primary source from which all design recommendations for tubular joints are derived [20] . This come in the form of observational data recorded during experiments. Other objectives of undertaking experimental work include parametric studies to confirm design equations, correlation of numerical analysis techniques and so on. For a tubular joint, there are three basic design criteria which are considered;

1. Static strength
2. Fatigue performance
3. Local joint behavior (stress distribution and local joint flexibility)

The selection of the appropriate modelling and testing techniques is dependent on both the objectives as well as the design criteria to be evaluated. There are three primary experimental techniques for modelling tubular joints; steel modelling technique, acrylic and araldite modelling techniques. while the latter two techniques are only suitable for establishing local joint behaviour, the steel modelling technique is suitable for all design problems. In essence, the stress concentration problem can be studied using any of the aforementioned techniques. Strain gauges are used to obtain the strain and stress distribution around the joint intersection. A special extrapolation gauge is placed according to the location of the peak stress. This type of tests are performed using suitable test rigs that apply special constraints to the joints. Figure 2.12 below gives an illustration of an experimental set up.



Figure 2.12: Tubular T-joint test. [8]

2.5.2 Simple joints SCF equations

This is a computational technique developed by researchers which give designers a most convenient way to estimate the hot-spot stress in simple tubular joints. These equations were reported at different points in time, utilizing different approaches in the definition and calculation of hot-spot stresses. There are also noticeable differences in their recommended ranges of applicability. Some of the most commonly used parametric equations are described under this section.

Kuang equations

The Kuang equations were reported in 1975-1977, utilizing a modified thin shell finite element program specifically designed to analyse tubular connections. These equations cover T/Y, K and KT joint configurations. In the Kuang formulation, tubular connections were modelled without a weld fillet, and stresses were measured at the mid-section of the member wall. The validity range for these equations is illustrated by table 2.1 below.

Lower limit	Parameter	Upper limit
6.66	α	40.0
0.3	β	0.80
8.33	γ	33.3
0.2	τ	0.80
0.00	θ	90.0
0.01	ς	1.0

Table 2.1: Validity range for Kuang equations

Wordsworth and Smedley equations

These equations were reported in 1978 and 1981 by Wordsworth/Smedley, using acrylic model test results on tubular joints modelled without a weld fillet. The first set of equations were reported by both researchers in 1978 covering T/Y and X joint configurations. And in 1981, Wordsworth reported another set of equations covering the K and KT joint configurations. These parametric equations adequately cover the crown and saddle, however it is unclear if interim sets of gauges were adopted, particularly under IPB where for some configurations the hot-spot stress occurs between the saddle and crown [18]. The validity range for these equations is illustrated in table 2.2 below;

Lower limit	Parameter	Upper limit
8	α	40.0
0.13	β	1.0
12	γ	32
0.25	τ	1.0
30.0	θ	90.0
N.A	ς	N.A

Table 2.2: Validity range for Wordsworth/Smedley equations

Efthymiou/Durkin equations

These series of parametric equations were published by Efthymiou and Durkin in 1985. They cover T/Y and gap/overlap K joint configurations. In 1988, Efthymiou published an update of simple joint parametric equations covering T/Y, X, K and KT simple joint configurations. Efthymiou's equations are found in popular design standards such as DNV-RP-C203, BS-EN ISO 19902 etc. These equations were derived using influence functions to describe K, KT and multi-planar joints in terms of simple T braces with carry-over effects from the additional loaded braces [18]. Their validity range is illustrated by table 2.3 below;

Lower limit	Parameter	Upper limit
4.0	α	40.0
0.2	β	1.0
8.0	γ	32.0
0.20	τ	1.0
20.0	θ	90.0
$-0.6\beta/\sin\theta$	ς	1.0

Table 2.3: Validity range for Efthymiou/Durkin equations

2.5.3 Finite element method FEM

One of the major applications of finite elements analysis in the offshore industry is the determination of stress concentration factors (SCF) for the purpose of fatigue analysis. According to [15], a finite element analysis may be required in tubular joint design cases where stress concentration factors are not adequately predicted by the standard parametric formulae, or where greater confidence is needed in the results. Application of FEA involves the use of a finite element analysis (FEA) software, and it begins with a computer aided design (CAD) model of the part been simulated, a knowledge of the material properties making up the structure, as well as the applied loads and boundary conditions. As opposed to experimental method, FEA provides the means to explore a wide range of design options quickly and cheaply, allowing the prediction of solutions to real problems with often high accuracy. However, the accuracy of results obtainable is largely dependent on the skill of the user. In this project, a finite element analysis of simple tubular joints will be carried out using the FEA software Abaqus/CAE, also known as complete Abaqus environment. Abaqus is used for both pre-processing (modelling and analysis) as well as post-processing or visualisation of analysis results. The upcoming sections will go through the relevant theoretical concepts involved in the finite element modelling of tubular joints.

Stress theories

This section aims to discuss some of the most common stress theories applied in the investigation of stress concentration in tubular joints. Most finite element software can extract a wide range of stresses and from any part of choice in a model. However, the most common stress results used for analysis are the principal stresses and the Von Mises stress. Depending on mechanical properties of the material, analysts choose which one of the two stresses is more suitable. For example, when looking at brittle materials, analysts choose maximum principal stress. While Von Mises stress is preferred for linear static analysis of ductile materials such as steel. However, maximum principal stress is often used in fatigue analysis of ductile and brittle materials. It should also be noted that the direction of the principal stresses do not always align with the FE software coordinate, and that they could be at any angle. In summary, the principal stress vector contours gives a useful indication of the flow of stresses, while the Von Mises stress is used as an overall indicator of stress distribution and stress concentration location, which is the subject of this study. Therefore, the Von Mises stresses will be used to quantify stress concentration in this study.

Element formulations for FEM

A number of element formulations are available for the analysis of tubular joints, ranging from flat plate elements to solid elements. Curved shell elements are widely used and they provide a good balance between accuracy and economy. According to DNV-RP-C203, the arrangement and type of elements (element formulation) in FE modelling of tubular joints have to allow for steep stress gradients as well as for the formation of plate bending. And conversely, only the linear stress distribution in the plate thickness direction needs to be evaluated with respect to the definition of hot spot stress. In essence, both 2D shell elements and 3D solid elements are commonly used for FE analysis of tubular joints. The choice of element type for analysis depends on the geometry of the joint and the purpose for which the results are needed. It can be said to be a compromise between the accuracy of representation and the computation time necessary. These two options are further described below.

Shell elements

Shell elements are used to represent parts that are thin compared to their area dimension, i.e. one dimension is much smaller than the other two. They are either defined as four sided elements known as quadrilaterals or three sided elements commonly known as tris. Shell elements are physically represented as surfaces, and their thickness is determined by a user-defined property on the FEA software. This presents a great benefit in the use of shells since a change in thickness does not require any CAD or geometry changes. Abaqus shell element library provides a wide range of elements that are broadly categorized into thin, thick and general purpose shell elements. Shell elements are suitable for solving the elastic structural stresses according to the shell theory. Using these shell elements, tubular joints are modelled as intersecting cylindrical tubes at the mid-surfaces of the walls. Where the mid-plane stress is equal to the membrane stress, and the top and bottom surface stresses are superimposed membrane and shell bending stresses. Since thin shells can only model the mid-planes of the tube because material thickness is only a property of the element, the weld is not modelled and some details of the 3D stresses are lost. This leads to hot spot stress locations which are different to steel models and the same reason why there are some differences between results obtained using FE shell modelling and the those obtained using steel models [3].

Solid elements

Solid elements are volume elements filling a defined volume. They are defined as six-sided hexahedrons, known as bricks or hexes, five-sided triangular prisms known as wedges or pentas, four-sided solids called tetrahedrons, often called tets or square pyramids which allow for transitions between hex and tet meshed areas. These types of elements can be used to model tubular joints including the weld toe profile which could be modelled as a sharp notch. And because of this, models using solid elements provide more accurate and detailed stress behavior near the intersection. These element types are also useful in applications that require more detailed information in the intersection such as fracture mechanics studies of defects in tubular joints.

Summary

In summary, the following considerations are given by [16] regarding finite element modelling of tubular joints in order to obtain hot spot stress.

- Element type: Linear elastic quadrilateral plate or shell elements are typically used, with mesh created at the mid level of the plate and without representation of the weld profile in the model. In special situations where the weld effect brings about changes in the analysis results e.g. in cases where the results are affected by high local bending, solid elements are preferable. However a use of triangular elements in the hot spot region is discouraged.
- Element size: The element size around the hot spot region should be approximately $t \times t$, where t is the thickness of the shell. For 8 noded shell elements, mesh size up to $2t \times 2t$ may be used.
- Aspect ratio: An aspect ratio of 1:1 should be used immediately adjacent to the hot spot location. It should ideally be limited to 1:3 and should not exceed 1:5. The aspect ratio of the shell element represents the ratio of its arbitrary length to width.
- Gradation of mesh: The mesh is expected to get finer towards the hot spot region and coarser away from it, in a smooth and uniform fashion. It is also suggested that several of the elements leading into the hot spot location should be the same size.
- Stress of interest: The hot spot stress approach utilizes a linear extrapolation of relevant stress at two locations adjacent to the hot spot stress location, to the actual hot spot.

2.6 Fatigue life evaluation

This section will cover relevant concepts and methods used for fatigue assessment in tubular joints. The fatigue performance of tubular joints is of primary importance to the integrity of offshore jacket structures. Poor fatigue performance is marked by large stress variations in hot spots, and the high residual stresses and defects introduced by welding, this combination can ultimately lead to fatigue failure. Fatigue assessment refers to a process whereby the fatigue demand on a joint is established and compared to its predicted fatigue strength. Fatigue assessment techniques are categorized either based on a direct calculation of fatigue damage or expected fatigue life. In this project, fatigue assessment based on expected fatigue life will be considered. There are two most basic approaches to the fatigue life assessment of tubular joints. The S-N approach which depends on empirically derived relationships between applied stress ranges and fatigue life and a second approach which is based on linear elastic fracture mechanics. There is also a more advanced approach based on damage accumulation. This approach is more commonly known as the Palmegran-Miner rule and is mentioned in several industry standards including DNV-RP-C203. The following sections discuss these approaches.

2.6.1 The S-N Approach

The S-N approach is the most widely used approach for the fatigue life assessment of tubular joints. As mentioned earlier, it relies on empirically derived relationships between applied stress ranges and fatigue life. As such, it presents the fatigue strength of tubular joints as a curve representing the number of cycles that will cause fatigue failure. Within the S-N approach, several other methods exist. These methods are mainly distinguished by the parameters used to describe fatigue life 'N'. These methods include the nominal stress method, the hot spot stress method, the notch intensity approach etc. This further classification makes it important that stresses are calculated in agreement with the definition of stresses to be used with particular S-N curves. For example, in order to derive the fatigue life using the hot spot stress method for tubular joints under multi-axial loading conditions, 8 points around the periphery of a tubular joint are usually considered. SCFs are obtained at each of these points and multiplied with the nominal stress range to obtain the hot spot stress range. The calculated hot spot stress is entered in a hot spot S-N curve for derivation of fatigue life. Notch stresses due to local weld geometry is excluded from the stress calculations since they are assumed to be accounted for in the hot spot S-N curve. It is important to note that the derivation of the stress range depends on the type of loading to which the joint is subjected to, for a joint under multi-axial loading, the procedure using 8 points around periphery is applied, while for a case of uni-axial loading, the largest hot spot stress around the joint can simply be used as can be seen later in this report.

But more generally, two types of S-N curves are observed from fatigue tests of different materials. Certain materials like most ferrous and titanium alloys exhibit a distinct limit known as the endurance limit, this means that there is a stress level below which an infinite number of loading cycles can be applied without causing fatigue failure. On the other hand, many non ferrous materials and alloys such as aluminum, and magnesium alloys do not show such defined limits, they instead display a continuously decreasing S-N response. Because of that, the term endurance strength is used to measure fatigue life. Both curves are illustrated using figure 2.13 below.

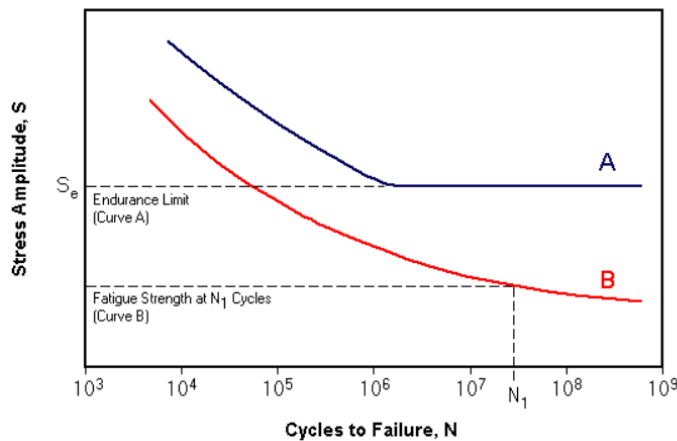


Figure 2.13: Typical S-N curves [13] .

One of the major shortcomings of this approach is that it cannot be used to assess the structural integrity of cracked tubular joints in service. Which is where fatigue analysis based on fracture mechanics comes in as a supplement to S-N data. Fracture mechanics uses the Paris equation to predict crack propagation or fatigue life in a welded detail. The Paris law relates crack propagation, fatigue life to the stress intensity factor. Fracture mechanics is recommended for use in assessment of acceptable defects, evaluation of acceptance criteria for fabrication and for planning in-service inspection. The approach is said to report shorter fatigue life than the S-N approach since crack initiation is not normally included in deriving the solution. It is also important that there is available S-N data to verify assumptions made in deriving solutions using fracture mechanics. The fracture mechanics approach will not be further discussed since it is not relevant to this study.

Stress analysis of simple tubular joints

3.1 Stress concentration factors by design code

This section covers the methodology as well as the computation work carried out in order to obtain the stress concentration factors, hot spot stresses, as well as the fatigue life(s) of simple tubular T-joint using DNV-RP-C203. The joint will be checked for stress concentration under the 3 basic loading modes namely; Axial loading, in-plane and out-of-plane bending. Several other standards such as BS-EN ISO19902 and API RP-2A WSD have referenced stress concentration in such a joint but the DNV recommended practice will be utilized here.

3.1.1 Stress concentration factor SCF

Stress concentration in DNV-RP-C203 is defined through stress concentration factors derived from parametric equations. The parametric equations to be used in calculating SCFs are reported by Efthymiou, reference can be made to section 2.5.2 of this report. These equations as found in the standard were prescribed for different joint configurations under different boundary conditions, as well as having defined ranges of applicability. In order to compute SCFs using these equations, it is necessary to carry out a detailed classification of the joint as well as checking for the validity of the set of equations in relation to the joint under consideration. After establishing validity, SCFs are then calculated at different locations around the joint. Figure 3.1 illustrates the joint under consideration, where positions indicated 1 and 2 are called the crown and saddle positions respectively. The location at which most stress concentration is likely to occur depends on the loading mode as can be seen by the choice of locations checked. It should also be noted that SCF equations in the standard are only presented for crown and saddle positions.

For the T-joint considered in this section, the joint parameters as well as their validity with respect to the referenced equations are presented under table 3.1 below. A more

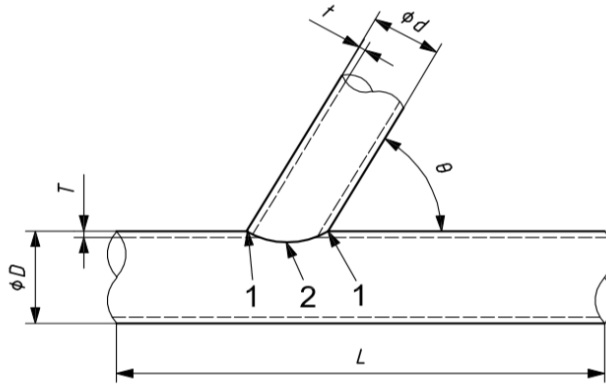


Figure 3.1: T or Y-joint [9] .

symbolic definition of the parameters can be seen in the appendix of this report. The same reference also shows the equations with are used to determine SCFs at chord/saddle positions under different loading conditions as specified by DNV-RP-C203. As shown by table 3.2, SCF_{AC} represents the stress concentration factor for the T-joint under axial compression while SCF_{IPB} and SCF_{OPB} represent the stress concentration factors under in-plane and out-of-plane bending respectively. All stress concentration factors were calculated assuming fixed boundary conditions on the chord ends. These values are later compared with SCFs obtained using FEA software Abaqus/CAE.

Table 3.1: Geometric parameters for the joint under consideration.

Parameter	Value	Validity/Efthymiou
α	5.087	OK
β	0.5205	OK
γ	27.38	OK
τ	0.75	OK
θ	90 degrees	OK
ς	N.A	OK

Table 3.2: Stress concentration factors using DNV-RP-C203.

Location	SCF_{AC}	SCF_{IPB}	SCF_{OPB}
Brace saddle	7.960	-	10.14
Brace crown	1.290	3.95	-
Chord saddle	12.66	-	13.63
Chord crown	3.300	5.010	-

3.1.2 Fatigue life estimation

Fatigue life evaluation is performed using the S-N approach. DNV-RP-C203 recommends a particular S-N curve for tubular joints known as the T-curve. This curve covers tubular joints in both air and seawater conditions under cathodic protection as illustrated by figure 3.2. The fatigue life of a joint is simply read on the curve using the corresponding stress range to which it is subjected. In a single action loading case, the stress range is the same as the highest hot spot stress recorded under the load. In this case, the loads are applied differently, each at a single step, therefore each loading case will have a single relevant hot spot stress that can be considered for fatigue life evaluation. Depending on the size of the stress range it can be determined whether or not the fatigue life can be read from the S-N curve, In cases where the stress range is not represented by figure 3.2, Equation 3.1 is used to determine the fatigue life. This equation is defined in relation to parameters in table 3.3. The stress range applied in this case is covered by the S-N curve but accurate reading can be difficult, so the fatigue lives are calculated using Equation 3.1 and the results are shown in table 3.4.

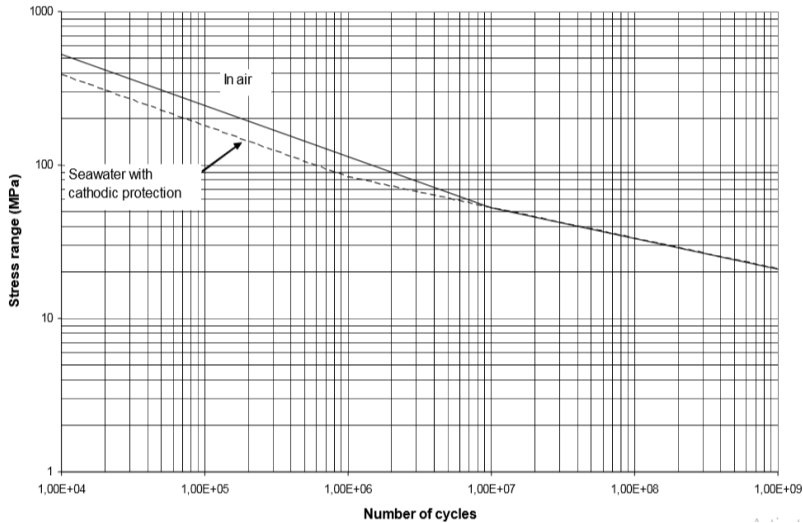


Figure 3.2: S-N curve for tubular joints in air and in sea water under cathodic protection. [7]

$$\log N = \log \bar{a} - m \log \left(\Delta \sigma \left(\frac{t}{t_{ref}} \right)^k \right) \quad (3.1)$$

where; N = predicted number of cycles to failure for stress range $\Delta \sigma$

$\Delta \sigma$ = Stress range

m = negative inverse slope of S-N curve

$\log \bar{a}$ = intercept of $\log N$ axis by S-N curve

t_{ref} = 32mm for tubular joints

t = thickness through which a crack will likely grow, $t = t_{ref}$ for thickness less than t_{ref}

The above parameters are defined by DNV-RP-C203 according to N by table 3.3.

Table 3.3: S-N curve for tubular joints in air DNV-RP-C203.

S-N curve	N ≤ 1.0 E +07		N > 1.0 E +07		Thickness component
	$\log \bar{a}_1$	m_1	$\log \bar{a}_2$	m_2	
T	12.164	3	15.606	5	0.25 for SCF ≤ 10 0.3 for SCF ≥ 10

Table 3.4: Fatigue life estimation using DNV-RP-C203.

Load/Location	SCF	Stress range [MPa]	Fatigue life (cycles)
Axial-Chord saddle	12.67	127.0	7.172E +05
IPB-Chord crown	5.010	50.10	1.160E +07
OPB-Chord saddle	13.63	136.0	5.761E +05

3.2 Stress concentration factors by Abaqus CAE

This section covers the steps involved in determining stress concentration factors using finite element software Abaqus/CAE. The aim here is to use finite element analysis FEA to determine the hot spot stress and then use the applied nominal stress in order to compute SCFs. FEA provides a more convenient alternative for calculation of fatigue damage because in practice, it may be difficult to evaluate what is the nominal stress to be used together with the S-N curves, as some of the local stress due to a detail is accounted for in the S-N curves [7]. The method consists of 3 separate stages. Pre-processing which involves creating an input file for the FEA solver, processing or finite element analysis which produces an output visual file, and post-processing which involves reading and extracting results from the output. It is possible to carry out all stages in Abaqus/CAE. However, the Abaqus package is more powerful for executing the last two stages. In this project, all 3 stages were carried out in Abaqus/CAE. The Abaqus/Standard which is a general-purpose finite element analyzer that employs an implicit integration scheme as the solver is utilized. The next sections cover the stages involved through the finite element analysis. Refer to section 2.5.3 for more on the finite element method.

3.2.1 Part module

The tubular T-joint was modelled as a 3D deformable type, extruded as a shell section. The tubular joint comprised of brace and chord without the weld. The procedure described in 3.2.7 allows modelling of tubular joints as shells without modelling the weld as will be done here. Table 3.5 defines the geometric dimensions used for joint modelling, see figure 3.1 for illustration. The property module is used to define a material for the model, with mechanical properties as shown in table 3.6 below. The units are defined in accordance with Abaqus consistent units. Also the section is created and assigned separately for both brace and chord. While creating the sections, shell thickness for brace and chord were defined and the default Simpson rule with 5 integration points was selected. Material orientation was assigned to model top surface of the shell.

Table 3.5: Definition of joint parameters.

Parameter	Value
Chord diameter (D)	438 mm
Brace diameter (d)	228 mm
Chord thickness (T)	8 mm
Brace thickness (t)	6 mm
Brace-chord angle (θ)	90 degrees
Chord length (L)	1114 mm

Table 3.6: Material properties.

Property (structural steel)	Value	Unit
Elastic modulus	200000	kPa
Poisson ratio	0.3	-
Yield stress	180	MPa
Ultimate stress	380	MPa

3.2.2 Assembly module

The assembly module is used to create and modify the assembly. An assembly is made of instances of parts from the model. The role of the assembly is to allow positioning instances of parts relative to each other in a global coordinate system. The model in this case consist of a single instance of the T-joint, created as an independent part. The partition toolset is used to divide the T-joint into smaller regions as shown by figure 3.3 below. Partitioning allows the user to gain more control over mesh generation, this includes obtaining regions to which different element types can be assigned.

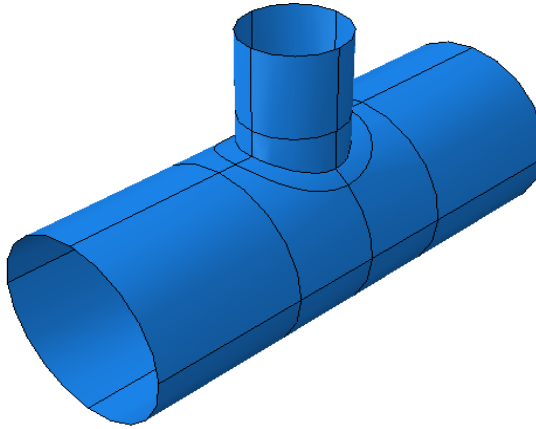


Figure 3.3: Instance of T-joint showing partitions.

3.2.3 Step module

The step module was used to create the steps involved in the analysis as well as to specify output requests. The step sequence provides a convenient way to define changes in the loading and boundary conditions of the model [1]. Abaqus/CAE automatically creates an initial step which will later be used to define boundary conditions. This is followed by three more steps each for the different loading modes namely, axial loading, in-plane and out-of-plane bending conditions. Each step is defined as a static general with a default increment size. Alternatively we could define three different models each containing one loading mode. Field output request in each loading cases is restricted to the relevant analysis step without allowing propagation to subsequent analysis steps. Figure 3.4 illustrates the definition of analysis step for the axial loading mode. The other two were defined in similar fashion.

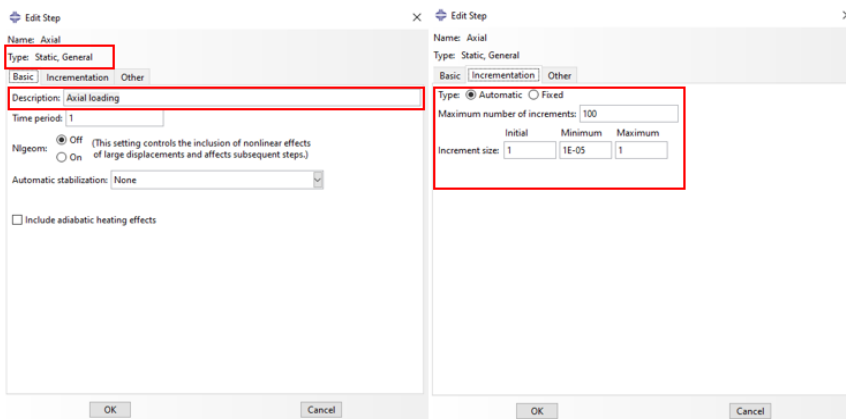


Figure 3.4: Defining analysis step for axial loading.

3.2.4 Interaction module

The interaction module was used to define analysis constraints between regions of the T-joint. This involved defining constraints for boundary conditions as well as region for the application of load. 3 multi point constraints (MPCs) were created, at each of the two chord ends and at brace end. The MPC constraints were defined as beam types with a master node at a reference point in the center of e.g. the chord, and slave nodes around the chord end. Beam MPCs provide a rigid beam between two nodes to constrain the displacement and rotation at the first node (at reference point) to the displacement and rotation at the second node (in the shell section), corresponding to the presence of a rigid beam between the two nodes [1]. Figure 3.5 shows the various constraints and their location. MPC chord L and R represent constraints for left and right chord ends respectively.

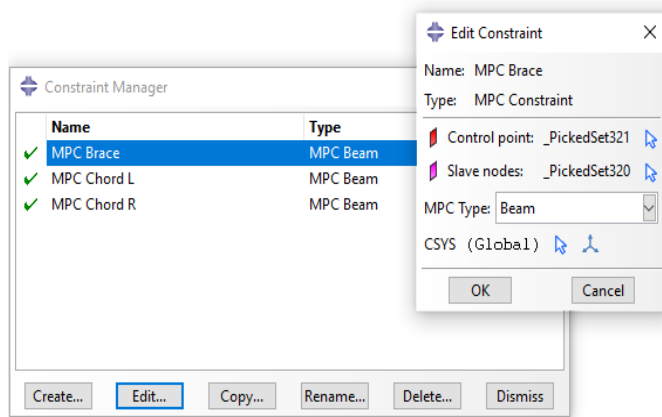


Figure 3.5: Constraints for application of load and boundary conditions.

3.2.5 Load module - Load and boundary condition

The load module was used for defining loads and boundary conditions. Each load was defined as a single action load in each of the three steps. Their step dependent feature was used to specify the steps in which they are active and vice versa. Loads were specified using already defined constraints from the interaction module. A concentrated force was used to define axial loading while concentrated moment was used to define both in-plane and out-of-plane bending. Figure 3.6 shows procedure for specifying axial load and table 3.7 shows the magnitudes of loading used for calculation of SCFs.

A fixed boundary condition was applied at chord ends allowing zero translational and rotational motions in all directions. Corresponding to the boundary condition specified for the parametric equations referenced in DNV-RP-C203. Figure 3.7 shows the definition of one of the boundary conditions.

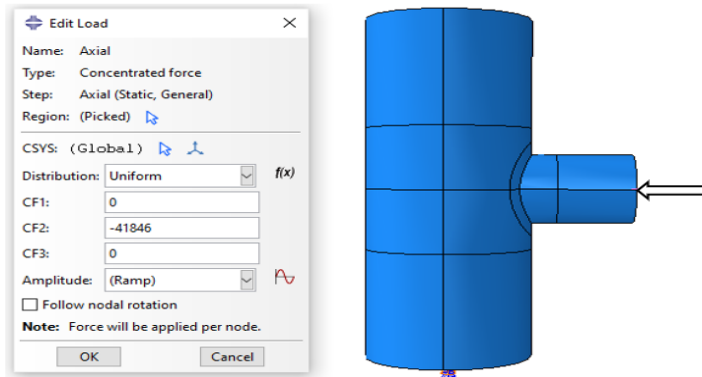


Figure 3.6: Definition of axial loading.

Table 3.7: Magnitude and direction of loads applied under different loading modes.

Loading type	X-direction	Y-direction	Z-direction
Axial [N]	-	-41846	-
In-plane bending [Nm]	2.32E+006	-	-
Out-of-plane bending [Nm]	-	-	2.32E+006

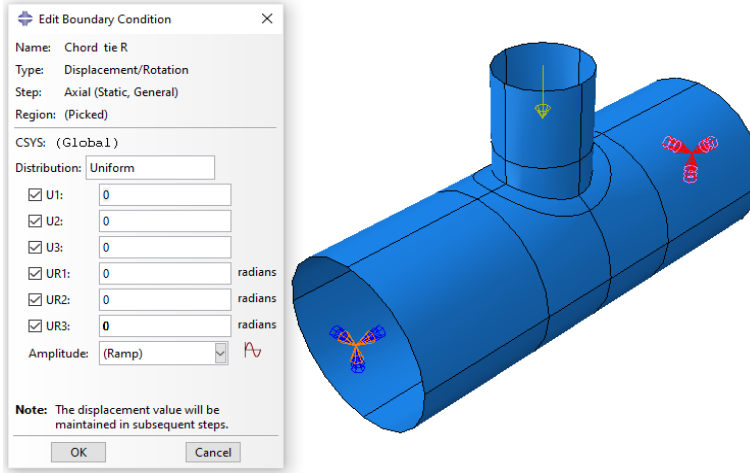


Figure 3.7: Definition of boundary conditions.

3.2.6 Mesh module

The mesh module was used to generate meshes on the T-joint instance. The mesh module provides a number of features including, tools for prescribing mesh density at local and

global levels, model coloring that indicates the meshing technique assigned to each region in the model. It also provides a variety of mesh controls such as element shape, meshing technique, meshing algorithm and adaptive remeshing [1]. The mesh density was specified by first applying global seeding on the T-joint instance and later applying local seeds on regions around which hot spot stresses are to be determined. Biased seeding was used where needed to ensure smooth variation as mesh density changes between regions. Mesh density is measured in millimeters. Figure 3.8 displays the seeding window as well as a seeded instance of the T-joint.

The element type window allows the user to select the element type that is assigned to the mesh by choosing the element family, geometric order, shape and other specific element controls. In this project, The main element used for meshing was the 8-noded, doubly curved thick shell element, otherwise known as the S8R element. The toolset provides several other options as can be seen in Figure 3.9 below, this includes the 4-noded thick shell element, but S8R element is recommended especially in case of steep stress gradients. This is specified in DNV-RP-C203. However, the S4R element is said to posses additional degrees of freedom for improved in-plane behaviour [7].

Mesh controls allows the user to choose the meshing technique which could be free, structured or swept. It is also possible to choose the meshing algorithm where applicable, this could be medial axis or advancing front. Abaqus/CAE automatically color codes the assembly according to which meshing technique could be used to mesh each region, In this case free meshing was indicated as meshing technique. Figure 3.10 shows the set data applied using the mesh control dialog. Lastly, mesh verification can be carried out to identify errors and warnings in the mesh and correct them.

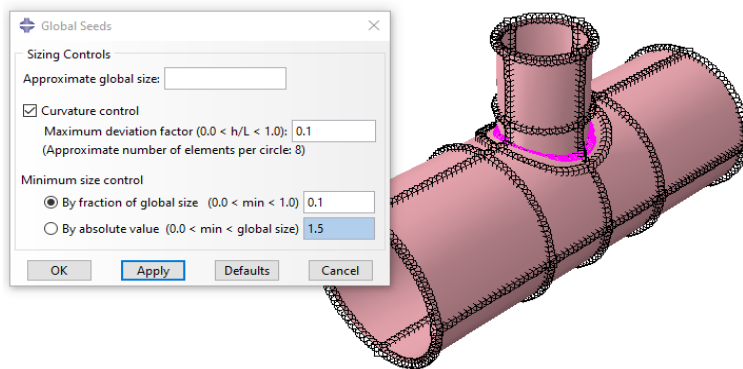


Figure 3.8: Seeding of part instance for mesh generation.

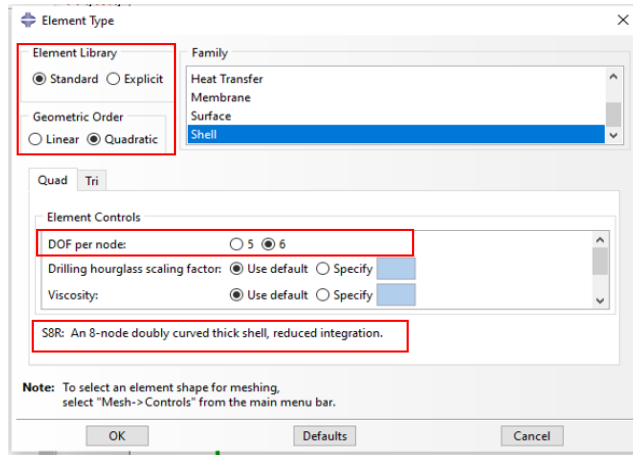


Figure 3.9: Element type window.

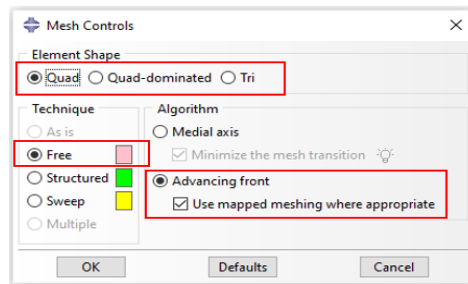


Figure 3.10: Mesh control window.

3.2.7 Derivation of hot spot stresses

The hot spot stress or geometric stress in tubular joints is calculated by a linear extrapolation of the stresses obtained from analysis at positions at distances a and b from the weld toe as indicated by Figure 3.11 [7]. a and b are known as the points for read out of stresses and are defined for the different locations as shown by equations 3.2-3.7. For joints other than tubular joints, stresses can be read at $0.5t$ and $1.5t$, where t is as defined in Figure 3.11.

For extrapolation of stress along the brace surface normal to the weld toe [7].

$$a = 0.2\sqrt{rt} \quad (3.2)$$

$$b = 0.65\sqrt{rt} \quad (3.3)$$

For extrapolation of stress along the chord surface normal to the weld toe at the crown position [7].

$$a = 0.2\sqrt{rt} \quad (3.4)$$

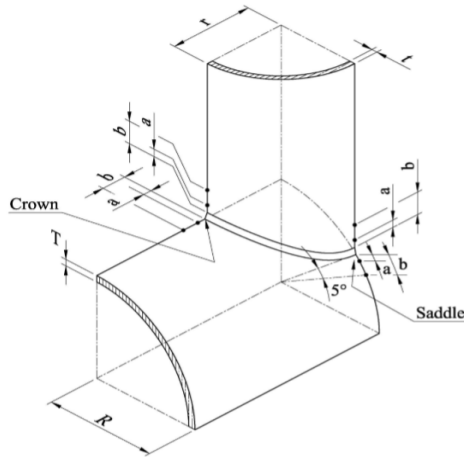


Figure 3.11: Points for read-out of stress for calculation of HSS [7] .

$$b = 0.4\sqrt[4]{rtRT} \quad (3.5)$$

For extrapolation of stress along the chord surface normal to the weld toe at the saddle position [7].

$$a = 0.2\sqrt{rt} \quad (3.6)$$

$$b = \frac{\pi R}{36} \quad (3.7)$$

It should be noted that, locations a and b are defined from the weld toe location and not from the brace wall. So in order to find out the extrapolation point, the distance from the weld toe to location a and b have to be determined, this is done according to the weld profiles shown in Figure 3.12 for both saddle and crown positions. Weld toe locations can be determined by checking the values of φ from each finite element model.

For ease of reading results, meshing can be adapted so that nodes are placed at a and b positions. This way, stresses at locations a and b can be directly extracted from the software and extrapolated to the weld toe in order to obtain the hot spot stress. Figure 3.13 shows an example of derivation of hot spot stress. This procedure allows the manual extrapolation of hot spot stresses from integration points. However, one should be mindful of the locations of the integration points when using this procedure. It should be noted that the illustration in Figure 3.13 is for plated structures not tubular joints.

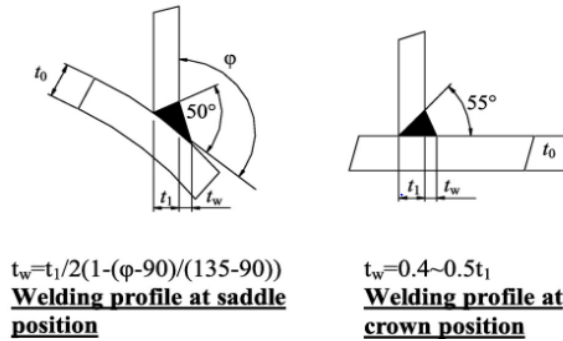


Figure 3.12: Welding profiles at both saddle and crown positions for determination of a and b locations. [23].

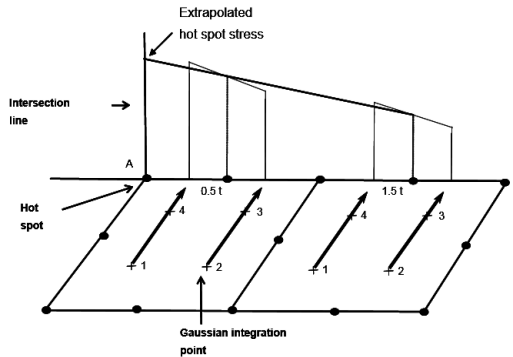


Figure 3.13: Example of derivation of hot spot stress. [7].

Shape functions are used to interpolate coordinates or displacements over an element. The interpolation provides a continuous field of the field quantity in question. Because stresses are extrapolated from the integration points to the side of an element, the shape functions can be used to carry out extrapolation within the element to the point of readout. This procedure is direct for the quadratic element (Q8 element, otherwise known as S8 in Abaqus/CAE) since it has a mid side node. But for the bi-linear quadrilateral element (otherwise known as Q4), it leads to more work for the analyst as the global coordinates of the corner nodes for the relevant element has to be found from the model and then extrapolation of stress components to the element sides can be performed. After reading stress at two points away from the weld toe, stress at the weld toe is determined by use of linear extrapolation. Figures 3.14 and 3.15 show the accompanying details for implementing this procedure. The procedure has not been utilized in this study.

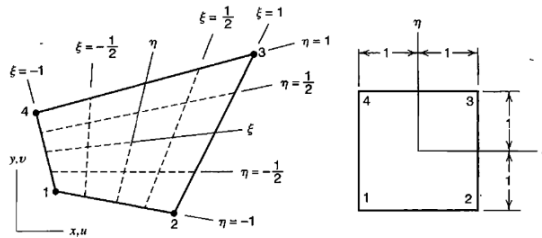


Figure 3.14: 4 node plane element in physical space (left) and the same element mapped into $\xi \eta$ space (right). [19] .

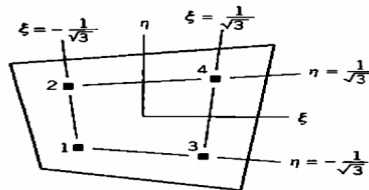


Figure 3.15: Sampling points for integration using Gauss rule of order 2. [19] .

3.2.8 Mesh convergence study

In order to verify the FE model and analysis procedure, a mesh convergence study is carried out. Mesh quality is known to affect the accuracy of results obtained from finite element analysis. Coarse meshes can yield inaccurate results therefore it is important to use a sufficiently refined mesh to ensure adequate results. In addition, this also ensures that adequate computational resources are used. The procedure involves the analysis of a single model with increasingly finer mesh and comparing the results. The numerical solution provided by the model tends toward a unique value as the mesh density is increased.

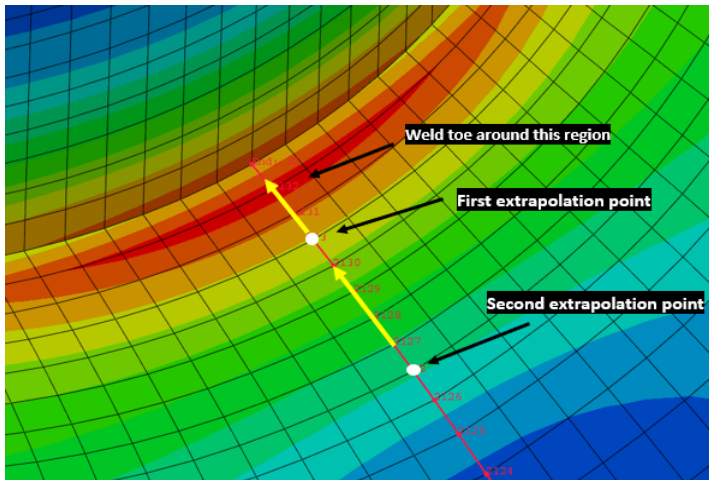
For the model presented under this chapter, φ has been measured from the model to be 121 degree, and weld toe locations are estimated using the pythagorean relation. The values are shown alongside values of a and b in table 3.8. Notice that the weld toe location estimated at the chord saddle position is quite small, therefore an assumed value of 3mm will be used as is the estimate for the crown position according to figure 3.12. All other values are used as estimated according to figure 3.12.

Extraction of analysis output was carried out as shown in Figure 3.16, illustrating the points of readout of stresses at the chord saddle. A path is created passing through points a and b , and the averaged Von Mises stress along the path is extracted. This data is plotted as shown by figure 3.17, alongside locations a , b as well as the weld toe. The crossing point between the linear extrapolation line and the weld toe line gives the hot spot stress. Analysis output can also be extracted directly at nodes by extracting nodal values

Table 3.8: Definition of points for readout of stresses and weld toe at different locations.

Position	Weld toe [mm]	a [mm]	b [mm]
Chord saddle	0.868, (Estimated)	6.099	19.979
Chord saddle	3, (Assumed)	8.231	22.11
Brace saddle	4.60	9.831	21.600
Chord crown	3	8.231	16.235
Brace crown	8.57	13.80	25.57

of stresses at a and b and then extrapolating the values to the weld toe.

**Figure 3.16:** Illustration of points for readout of stresses at the chord saddle position.

Mesh convergence is checked at the chord saddle using five different mesh qualities for S4R and the S8R elements. These elements use reduced integration when solving the integral and therefore require lower computation time. Reduced integration is the default Abaqus setting. However, it could have an effect on the accuracy of the element for a given problem. The effect of reduced and full integration is not investigated.

Mesh convergence was checked for the axial loading case at the chord saddle position. This is because tubular joints with loaded chord members will only be studied in the axial loading case, and focus will be mainly on the nature of stresses in the chord member.

Results shown in Figure 3.18 shows that SCFs determined using the standard are conservative compared to the FEA results. This is expected because the Efthymiou equations show a bias of up to about 10% to 25% on the conservative side when compared with FEA results [9].

Comparing results obtained using S4R and S8R elements, the S8R element seems to

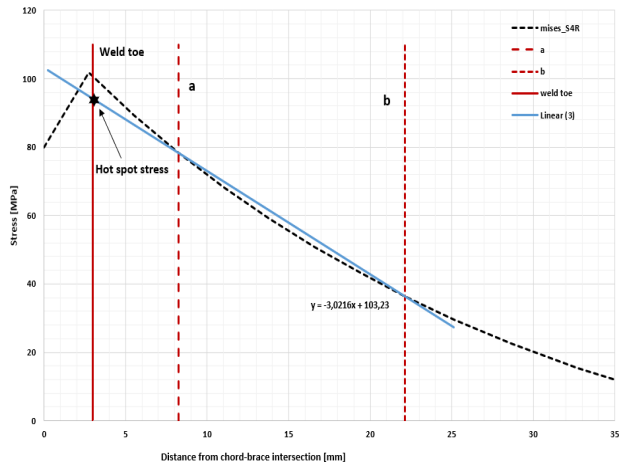


Figure 3.17: Derivation of hot spot stress.

converge faster, but results from both elements appeared to be tending towards a unique value as the mesh density increased. The difference in the manner of convergence comes from how the different elements are formulated in Abaqus/CAE, the S4R element has only one integration point per element, while the S8R has 4 integration points for every element, Abaqus stores results at these integration points and these results are then averaged to the nodes around the integration points. So the more the integration points, the closer the numerical solution gets towards convergence. Therefore it makes sense that the S8R element converged faster, and that the two elements tended towards the same value as the mesh density increased.

The eight-noded (S8) element is recommended by [7] particularly in case of steep stress gradients. And for this element, a mesh size from $t \times t$ up to $2t \times 2t$ may be used. Henceforth this recommendation will be used.

3.2.9 Stress concentration factors SCF

In order to determine stress concentration factors using FEA software Abaqus/CAE, procedures described and section 3.2.7 and implemented in section 3.2.8 were used. Hot spot stress was determined by linear extrapolation of stresses at a and b points, and then extrapolated to the weld toe. Read out points were defined as node sets to allow the extraction of unique nodal solutions from ODB field output. The averaged Von Mises stress at integration points was used as the field output for determination of hot spot stresses. Stress concentration factors were defined as a ratio of the hot spot stress to the nominal stress in the brace. A summary of the finite element modelling is presented in table 3.9. SCFs obtained for different locations under different loading cases are shown in table 3.10. The results are discussed under section 3.3.

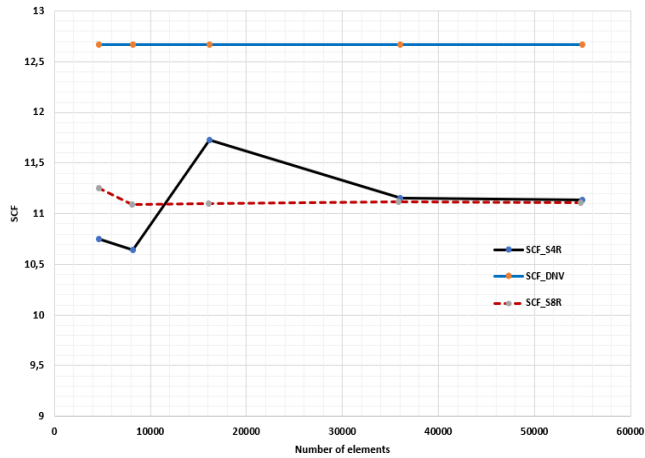


Figure 3.18: Estimated SCFs with respect to number of elements for S4R and S8R elements compared to the SCF from Eftymiou equations.

Table 3.9: Details for defining Abaqus/CAE model.

Property	Definition
Material behaviour	Linear elastic
Model body	Shell
Element type	8-noded thick shell element (Reduced integration)
Mesh refinement	t x t mesh around hot-spot areas
Weld	Not included
HSS for SCF calculation	Linear extrapolated stress from points of read out

Table 3.10: Stress concentration factors using Abaqus/CAE.

Location	SCF_{AC}	SCF_{IPB}	SCF_{OPB}
Brace saddle	8.090	-	9.158
Brace crown	1.053	1.680	-
Chord saddle	11.08	-	12.13
Chord crown	3.747	3.522	-

3.2.10 Fatigue life estimation

The fatigue life estimation was done in the same way as under section 3.1.1. The S-N approach as recommended by DNV-RP-C203 was used alongside the relevant S-N curve (T-curve) to determine fatigue life under different loading conditions. The main difference

to the procedure in section 3.1.1 is the manner in which the hot spot stress is determined, i.e. using the hot spot stress method as mentioned in 3.2.7. So in essence the fatigue life is only a function of the hot spot stress. The results are shown in table 3.11.

Table 3.11: Fatigue life estimation using Abaqus/CAE.

Load/Location	SCF	Stress range [MPa]	Fatigue life (cycles)
Axial-Chord saddle	11.08	110.8	1.072E +06
IPB-Chord crown	3.522	35.22	7.448E +07
OPB-Chord saddle	12.13	121.3	8.174E +05

3.3 Comparison of FEA and DNV results

FEA results demonstrate good agreement with results obtained using Efthymiou equations, with deviations of less than 20% except in the in-plane bending loading case where a deviation of up to 57% was recorded. The source of this deviation is suspected to be overestimation of the distance of extrapolation which resulted in a lower stress gradient. This will lead to lower stress region around this estimated weld toe, and thus result in a lower SCF.

The results of axial loading and out-of-plane bending agree with the assertion in ISO 19902 [9], which is according to the comparison studies by Lloyd's Register, that the Efthymiou SCF equations were found to provide a good fit to the screened SCF database, with a bias of about 10 % to 25% on the conservative side. Therefore the results are considered to be fairly accurate.

Even though results presented in table 3.13 show a quite considerable levels of deviation, they are still within the range of validity/accuracy expected of the FEA as compared to the Efthymiou equations with regards to fatigue life evaluation. This is deduced from the fact that the stress concentration factors used for determining the fatigue life(s) are within range of the accuracy achieved in comparison with the Efthymiou equations. This is ofcourse with the exception of the results estimated under in-plane bending.

Table 3.12: Stress concentration factors for T-joint using Abaqus and Efthymiou equations.

Axial loading			
Location	SCF_{abq}	SCF_{DNV}	Deviation[%]
Chord saddle	11.08	12.66	12 %
Brace saddle	8.090	7.960	2 %
Chord crown	3.740	3.300	12 %
Brace crown	1.053	1.290	18 %
In-plane bending			
Chord saddle	-	-	-
Brace saddle	-	-	-
Chord crown	3.522	5.010	30 %
Brace crown	1.680	3.950	57 %
Out-of-plane bending			
Chord saddle	12.13	13.63	11 %
Brace saddle	9.158	10.14	10 %
Chord crown	-	-	-
Brace crown	-	-	-
SCF _{abq} - SCF using Abaqus. SCF _{DNV} - SCF using DNV. Deviation - Percentage deviation between SCF _{abq} and SCF _{DNV}			

Table 3.13: Comparison between estimated fatigue life(s)

Load/Location	FL_{abq}(cycles)	FL_{DNV}(cycles)	Deviation
Axial-Chord saddle	1.072E +06	7.172E +05	33%
IPB-Chord crown	7.448E +07	1.160E +07	84%
OPB-Chord saddle	8.174E +05	5.710E +05	30%
FL _{abq} - Fatigue life using Abaqus stress range. FL _{DNV} - Fatigue life using DNV stress range.			

Stress analysis of simple tubular joints with loaded chord members

4.1 Introduction

This section covers the methodology and computation work carried out to determine stress concentration factors for the simple tubular joints with loaded chord members. The context of loaded chord member in this study shall be distributed circumferential vertical chord loading at different locations away from the crown position, in addition to axial brace loading. Illustration is given by figure 1.2. This context, as shall be discussed in the upcoming section has been largely unstudied. This study shall mainly focus on axial compressive loading on the brace, i.e. In-plane and out-of plane bending loads shall not be looked at. Also for the sake of perspective, vertical chord loads shall be defined as ratios of the axial compressive load on brace members.

A number of joint models will be investigated, where different magnitudes of chord load will be applied at different locations away from the crown position. For all models, focus will be on finding stress concentration factors on the chord side of the joint intersection as the effect of this type of loading is anticipated to be mainly on the chord member especially for the simple T-joint. This is further discussed in the next section. Also, fatigue life(s) are not calculated from stress concentration factors since they are only functions of the stress concentration factors for the type of loading used in this study.

4.2 Effect of chord stresses on SCFs

Different research projects have been carried out to investigate stress concentration in tubular joints with loads on the chord member, for example, [5] studied the effects of different boundary constraints and chord axial stresses on a K-configured joint. More closer to the objective of this thesis, [10] investigated bending effects on multi-planar welded tubular DT-joints. The study examined the effect of bending on both brace and chord members of

the joint. For chord bending, it was shown that chord crown locations exhibit significant stress concentrations, whereas SCF values at all other locations are negligible. However, it should be noted that the study only considered the chord load (axial or bending) as the only load from which stress concentration is determined, i.e. not chord load in addition to axial brace load as is considered in this study. ISO 19902 [9] also made a brief mention of the effects of nominal chord stress highlighting that nominal variable stress in the chord member contributes to stress ranges for fatigue damage accumulation, even though this contribution is small because chord forces do not cause any significant local distortion of the chord walls hence causing minimal stress raising effects. In the same standard, it was also pointed out that for T/Y joints, beam bending of the chord influences primarily the crown SCFs. This is in relation to the parametric equations reported by Effthymiuo. In essence studies have been carried out to investigate the effects of chord stresses on SCFs, although not exactly in the same context as this study, but it remains to be found how results from this study will compare to what is obtained in the literature.

4.3 Finite element modelling

Most of the steps involved in finite element modelling of the tubular joints with loaded chord members is covered in chapter 3, with few modifications on the loading and type of boundary condition used as described under the upcoming section.

4.3.1 Load Module - Load and boundary condition

In this section, definitions for loading and boundary conditions for the tubular joints with loaded chord member are outlined. Load on each model was a combination of a single action axial load on the brace as well as a distributed circumferential vertical load on the chord. The steps followed under section 3.2.5 for defining single action brace loads are similar to those applied here. vertical loads on the chord were defined as nodal loads, such that the total amount of load intended for the chord is divided by the number of nodes around the chord circumference and each unit applied on each of the nodes accordingly. This is illustrated by figure 4.1.

For all models investigated under this chapter, a pinned/hinged boundary condition will be utilized at chord ends. This is illustrated by figure 4.3. It is assumed that the effect of vertical chord loading might be more accurately captured using a hinge support instead of a completely rigid one. According to [11], the use of pinned boundary conditions led to higher SCFs at the crown position for the axial loading case. This will be kept in mind when evaluating the effects of the vertical chord loading on SCFs.

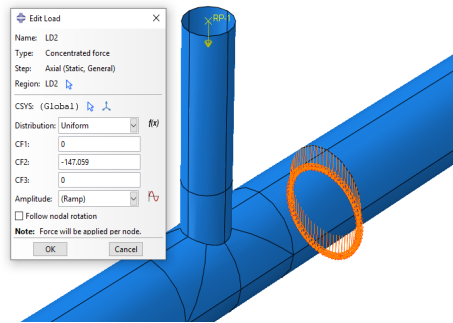


Figure 4.1: Illustration of application of chord load.

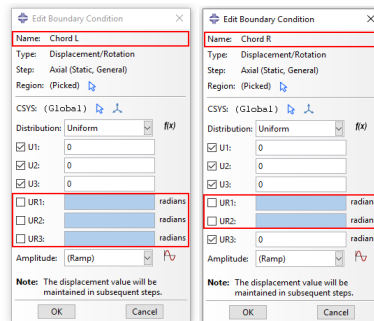


Figure 4.2: Boundary condition of model of left and right sides of chord member.

4.3.2 Checks for FEM models

In order to have confidence about the results obtained from finite element analysis of joints under this section, a few verification steps were carried out for each and every model.

- **Meshing** : Work has been put into ensuring that all meshes used are of sufficient quality. All meshes are carefully verified to discover any errors or warnings before submission for analysis. As much as possible element sizing was restricted to between $t \times t$ and $2t \times 2t$ as recommended by DNV-RP-C203 for the S8R element.
- **Reaction forces** : In Abaqus visualization module, reaction forces are checked at boundary conditions to ensure that they match the forces exerted on to the particular joint under consideration.
- **Field output contours** : In Abaqus visualization module, contours of field output variables such as displacements or stresses can be checked for any discontinuities. Discontinuities in field output contour may indicate a low quality mesh. For a good quality mesh, different averaging options should yield similar results. Figure 4.4 shows contour plots for an unconverged mesh using different averaging options. 50% and 75% showing different Mises stress at hot spot.

Another option is to use the Quilt-type contour plot for element based output which extrapolate values to element faces with no averaging, for this, only one color should be plotted per element to indicate a converged mesh.

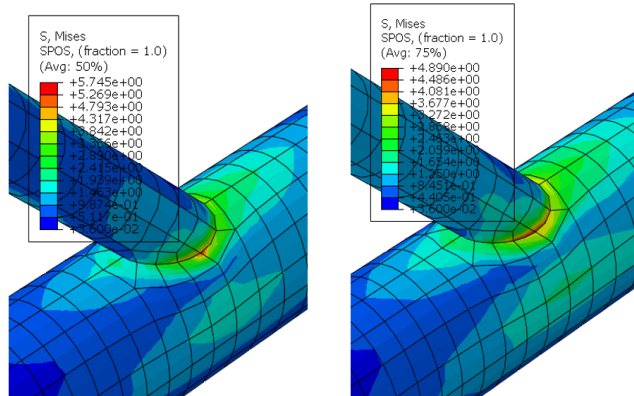


Figure 4.3: Contour plots for Mises stress using different averaging options.

- **Shell orientation** : Shell orientation is checked to ensure that results are extracted from the correct side of the element depending on the definition of the active section point.

4.3.3 Averaging of results in Abaqus

In Abaqus, stresses are calculated at integration points/element centroids, these points are inside each element. In order to determine the distribution of stresses over the entire model, values from integration points are extrapolated to nodes. Most nodes are common two more than one element, so they receive contribution from more than one element. The default setting in Abaqus is to compute results before averaging and then use 75% averaging threshold to average results from neighboring elements to obtain single scalar values for each node. 75% averaging means that if the relative difference between contributions coming to a node exceeds 75%, results are not averaged. 100% threshold averages all results, while 0% threshold does not average at all.

This provides an effective tool to quickly check mesh convergence, for the more sufficiently refined meshes, No difference should be noticeable between averaged and un-averaged results [6] . But on a more general basis, the closer the averaged results to the unaveraged, the more accurate the FEA results.

4.4 Stress concentration factors

In order to determine the stress concentration factors for the simple tubular T-joint with loaded chord members, parametric equations recommended by DNVGL-RP-C302 for general fixity conditions will be utilized. It should be noted that these equations were derived without considering any additional loading on the chord, so the loading condition in the finite element model is not exactly similar to that utilized in deriving the parametric equations. For the crown positions for both the brace and the chord, two equations were recommended, tagged equations 7a and 7b for the brace crown, and 6a and 6b for the chord crown. Equations 6a and 7a only provides correct hot spot stresses due to a single action load in the considered brace. While 6b and 7b provides correct hot spot stresses at the crown points under general loading conditions and moments in the chord member. Again, none of these recommended equations match the exact loading conditions of our finite element model, since we are considering a single action load on the brace in addition to distributed circumferential vertical load on the chord. Results from these equations will be used as a point of reference.

Since our finite element models are subjected to a single action load and only stress concentration factors on the chord side of the joint intersection are of interest, only equations 6a will be utilized.

4.5 Model I

This is a model of the simple T-joint with the same geometry as illustrated by table 3.5, and with geometric parameters within the validity range of the Efthymiou equations. For this model, a total of 9 cases were run, Utilizing 3 chord loading cases at 3 locations as shown by figure 4.4. The chord loading cases were defined as 1/8, 1/4 and 1/2 of the size of brace axial load, each loading case was applied one at a time at 3 different locations away from chord crown position, in this report, this is termed as the loading instance. Therefore for this model, 1/2, 1/4 and 1/8 represent the loading cases while SD1, SD2 and SD3 represent the loading instances. Each loading case has 3 loading instances. SD is the unloaded case. A summary of the FE model is shown in table 4.1.

With regards to the Efthymiou equations, this joint has a short chord as it has an $\alpha < 12$, This joint is investigated so it could be compared to a similar joint with a long chord according to this definition.

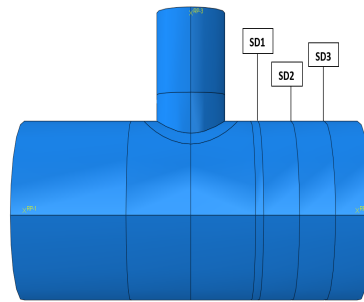


Figure 4.4: Illustration of partition lines for application of chord load.

Table 4.1: Summary of Model I

Tubular T-joint with short chord, $\alpha < 12$	
Element type	Shell, S8R
Method for read out of stress	a and b
Weld toe location	Assumed as 0.5t
Axial brace load	4184.6 N
Number of nodes around circumference	92
Nodal loads applied for 1/8,1/4,1/2 loading cases	5.686 N, 11.37 N, 22.74 N
Distances of chord load from crown position	110.75 mm, 221.5 mm, 332.25 mm

4.5.1 Results and observations

Stress concentration factors calculated are shown in table 4.2. These results are also plotted for better visualization as shown by Figures 4.6-4.8. Unit loads were used on the brace therefore the hot spot stress also represents the stress concentration factor. Figure 4.5 shows contour plots of Mises stresses for averaged and unaveraged results with slight deviation between the two, thanks to gradation of mesh towards the hot spot area. However, the two results are fairly close enough. The averaged results were used to compute SCFs.

For the chord saddle position, it could be seen that not much has happened, All extrapolation lines are effectively overlapping each other for all three loading cases. The SCF calculated using Efthymiou equations for such a joint is around 14.72, showing a 21% deviation between the standard and the unloaded case. There is no observable difference between loaded and unloaded cases. In fact, SCFs at this position is about the same for all cases run. Magnitude of chord load or its location did not seem to matter.

At the chord crown position, a consistent increase could be observed between loaded and unloaded cases as the magnitude of the distributed chord load increases. Starting from a 2 % deviation for 1/8 loading case up to a 7% deviation for the 1/2 loading case. With

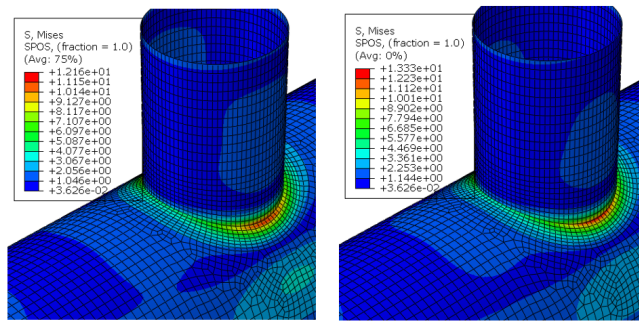


Figure 4.5: Contour plots for Mises stress showing averaged and unaveraged results.

Table 4.2: SCF from FEA T-joint with loaded chord member.

SCFs for load application at different locations away from the chord crown.						
Load case	position	SD	SD1	SD2	SD3	DNV
1/8 brace load	saddle	11.06	11.05	11.06	11.06	14.72
	crown	4.16	4.24	4.22	4.19	3.50
1/4 brace load	saddle	11.06	11.05	11.05	11.06	14.72
	crown	4.16	4.32	4.28	4.22	3.50
1/2 brace load	saddle	11.06	11.04	11.05	11.05	14.72
	crown	4.16	4.48	4.39	4.28	3.50

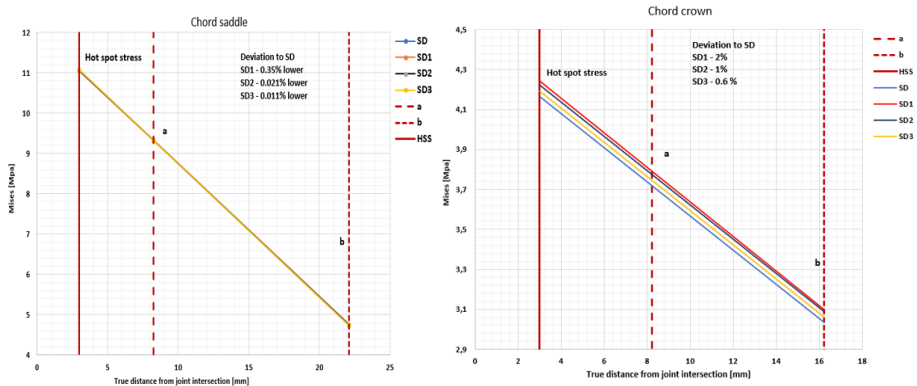


Figure 4.6: Extrapolation of stresses at point a and b to the hot spot for the 1/8 loading case.

the loading instances closest to the crown position showing the highest deviation from the unloaded case. In general, all loaded instances show effectively higher SCFs than the

unloaded case. SCF calculated from Efthymiou equation is 3.5, which as expected, is lower than all SCFs from the loaded cases. However chord loading does not account for all the difference between the two values, since the SCF from FEA for unloaded case is around 4.1.

Comparing the unloaded FEA case with DNV, it could be observed that SCF from DNV at the chord saddle position is conservative within expected range, while SCF from FEA at the crown position is on the conservative side. This is in agreement with the findings of [21] from a parametric study. Where they found that SCFs from the literature are not always conservative particularly at the crown of the chord.

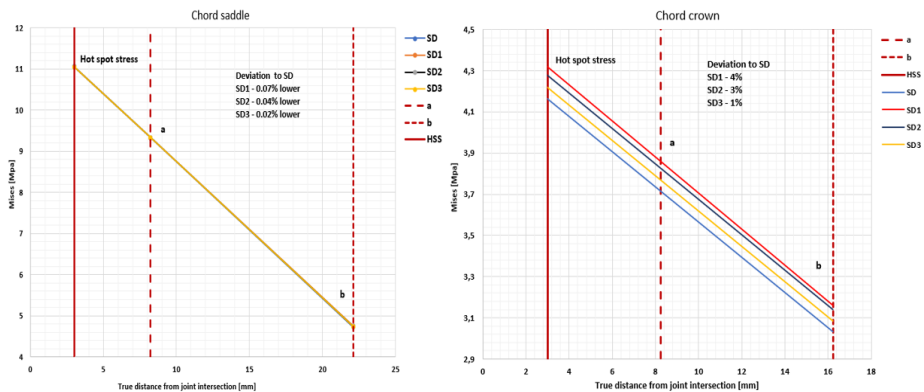


Figure 4.7: Extrapolation of stresses at point a and b to the hot spot for the 1/4 loading case.

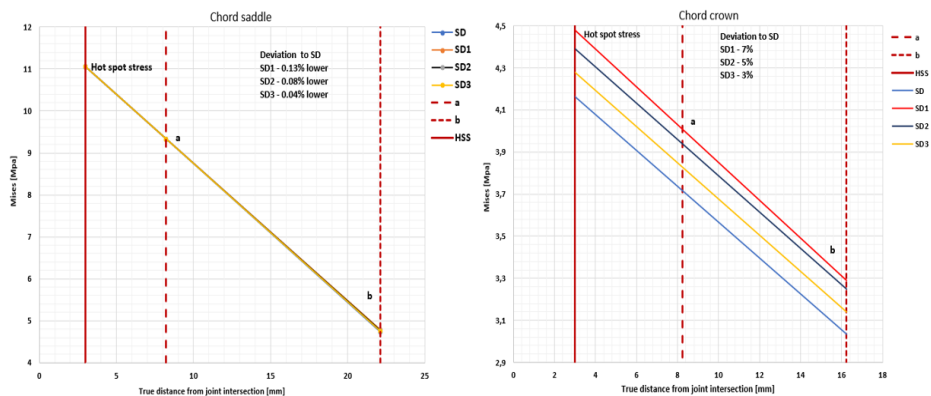


Figure 4.8: Extrapolation of stresses at point a and b to the hot spot for the 1/2 loading case.

4.6 Model II

The aim of this model is to check the effect of the chord length parameter α on the SCFs for T-joints with loaded chord members. The chord length for the joints modelled are defined to satisfy $\alpha > 12$ which is equivalent to $L > 6D$. Otherwise SCFs must be corrected using the Efthymiou short-chord correction factors. Nine joints were investigated utilizing three loading cases, and their geometry is defined by table 4.3. For this model, 1/2, 1/4, 1/8 represent the loading cases, while LD1, LD2 and LD3 represent the loading instances. LD is the unloaded case. All geometric parameters are within range of validity of the Efthymiou equations. A summary of the FE model is shown by table 4.4.

Table 4.3: Definition of joint geometry.

Parameter	Chord	Brace
Length	4658 mm	1000 mm
Outer diameter	438 mm	228 mm
Thickness	8 mm	6 mm

Table 4.4: Summary of Model II

Tubular T-joint with long chord, $\alpha > 12$	
Element type	Shell, S8R
Method for read out of stress	a and b
Weld toe location	Assumed as 0.5t
Axial brace load	4184.6 N
Number of nodes around circumference	68
Nodal loads applied for 1/8,1/4,1/2 loading cases	7.691 N, 15.38 N, 30.76 N
Distances of chord load from crown position	553.75 mm, 1107.5 mm, 1661.25 mm

4.6.1 Results and observations

SCFs calculated from FEA results are shown by table 4.5. These results are plotted as shown by Figures 4.9-4.11 for ease of visualization. Unit load is used on the brace so the hot spot stress also represent the SCF. Figure 4.9 shows contour plots of Mises stresses for averaged and unaveraged results with effectively no difference between the two results indicating a fully converged mesh. Here both results could be used to compute SCFs but the averaged result was used for consistency.

At the chord saddle position, the same pattern (as in Model I) is observed for the effect of chord loading on SCF. No visible deviation is recorded between the unloaded case and

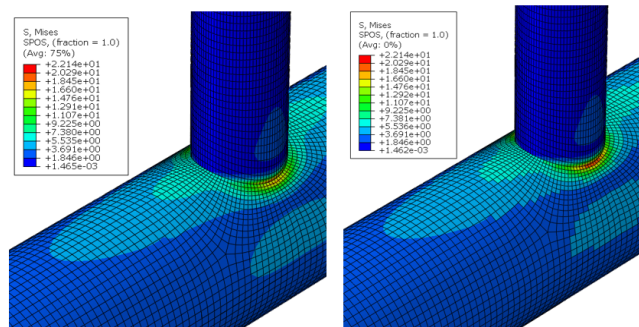


Figure 4.9: Contour plots for Mises stress showing averaged and unaveraged results.

Table 4.5: SCF from FEA T-joint with loaded chord member.

SCFs for load application at different locations away from the chord crown.						
Load case	position	LD	LD1	LD2	LD3	DNV
1/8 brace load	saddle	20.35	20.35	20.35	20.34	22.14
	crown	6.03	6.03	5.90	5.77	5.71
1/4 brace load	saddle	20.35	20.36	20.34	20.34	22.14
	crown	6.03	6.41	6.15	5.90	5.71
1/2 brace load	saddle	20.35	20.39	20.37	20.35	22.14
	crown	6.03	7.18	6.67	6.15	5.71

the different loaded instances, with all the extrapolation lines effectively overlapping each other. It can be said that the difference in chord length has no effect on the result of chord loading. But generally, an increase in chord length has the effect of increasing the SCF as is shown by the results.

At the chord crown position, the effect of chord loading seems to be gradually manifesting as the size of the load increases, For the 1/8 loading case, some of the loaded instances show a slightly lower SCF than the unloaded case, which is not expected. It is unclear why there is a dip in SCF, this seem to even out as the size of the chord load increased. Showing a more logical result in the 1/2 loading case, whereby the highest deviation from the unloaded case has increased to about 16% for the LD1 loaded instance. Based on this, chord length can be said to have an effect of increasing SCF at the crown position.

Comparing unloaded FEA case and DNV results shows the same pattern as observed in Model I. SCF from DNV at chord saddle position not quite as conservative as in Model I but still conservative. While SCF from FEA at the chord crown is yet the result on the conservative side. Once again agreeing with [21].

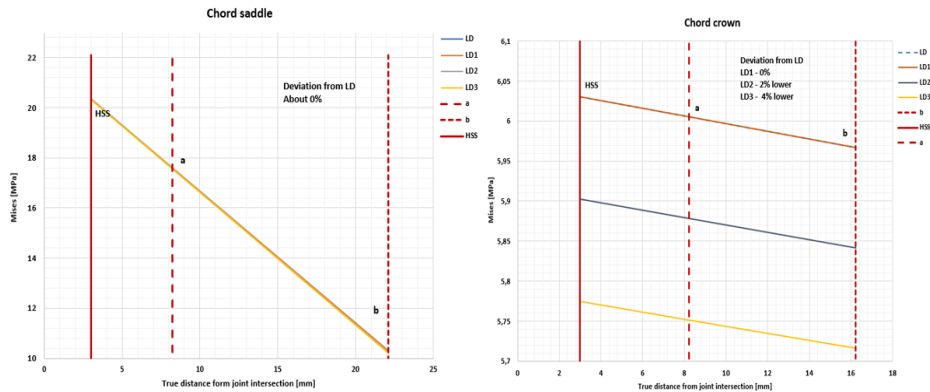


Figure 4.10: Extrapolation of stresses at point a and b to the hot spot for the 1/8 loading case.

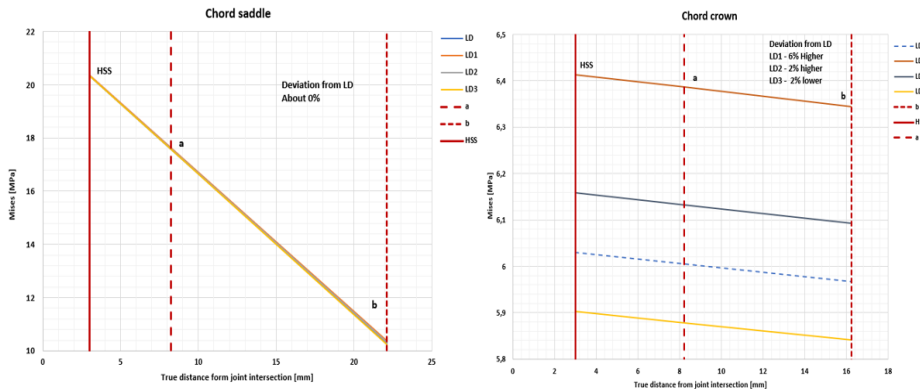


Figure 4.11: Extrapolation of stresses at point a and b to the hot spot for the 1/4 loading case.

4.7 Model III

The aim of this model is to check the effect of the diameter ratio of the brace and the chord on SCFs. 9 models were investigated where, 1/2, 1/4, 1/8 represent the loading cases, and PD1, PD2 and PD3 represent the loading instances. PD is the unloaded case. The T-joints used for the model are defined with long chord member with reference to the Efthymiou equations, satisfying $L > 6D$. Their geometry is defined by table 4.6, and a summary of the FE model is shown by table 4.7.

4.7.1 Results and observations

SCFs calculated from FEA are shown by table 4.8. These results are also plotted as shown by figures 4.14-4.16 for better visualization. On these figures, hot spot stresses also rep-

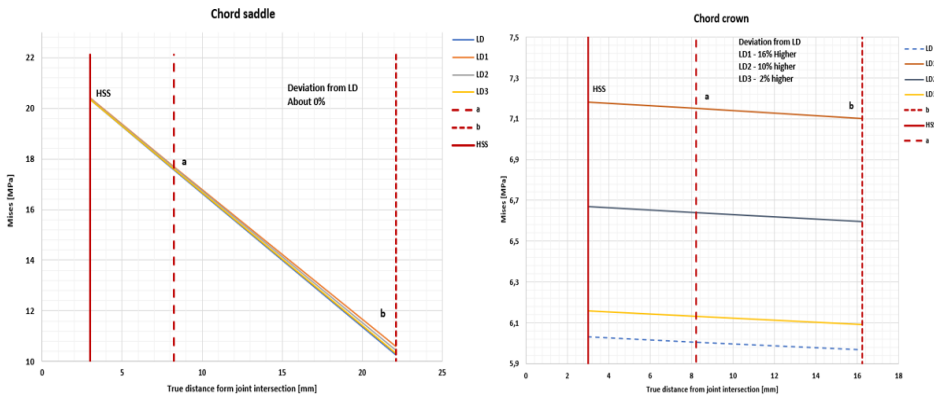


Figure 4.12: Extrapolation of stresses at point a and b to the hot spot for the 1/2 loading case.

Table 4.6: Definition of joint geometry.

Parameter	Chord	Brace
Length	4658 mm	965 mm
Outer diameter	508 mm	406.5 mm
Thickness	7.987 mm	7.828 mm

Table 4.7: Summary of Model III

Tubular T-joint with long chord, $\alpha > 12$	
Element type	Shell, S8R
Method for read out of stress	a and b
Weld toe location	Assumed as 0.5t
Axial brace load	9803.89 N
Number of nodes around circumference	82
Nodal loads applied for 1/8, 1/4, 1/2 loading cases	14.94 N, 29.89 N, 59.78 N
Distances of chord load from crown position	531.44 mm, 1062.87 mm, 1594.31 mm

resent SCFs since unit stress was applied on the brace. Figure 4.13 shows contour plots of Mises stresses for the averaged and unaveraged results with some level of deviation between the two. However, this deviation is not quite pronounced. The averaged results were used to compute SCFs.

At the chord saddle position, the effect of chord loading on the SCF is quite negligible, similar to what is recorded in Models I and II. Looking at the results in table 4.8, there is

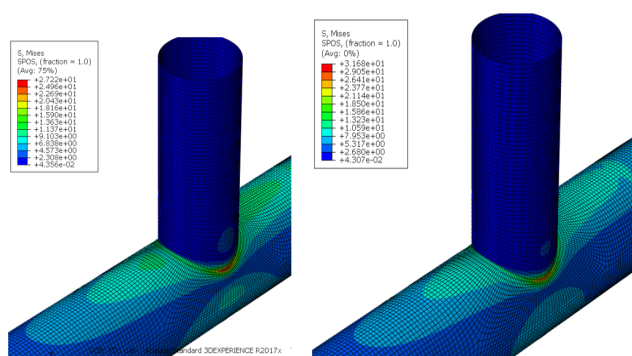


Figure 4.13: Contour plots for Mises stress showing averaged and unaveraged results.

Table 4.8: SCF from FEA T-joint with loaded chord member.

SCFs for load application at different locations away from the chord crown.						
Load case	position	PD	PD1	PD2	PD3	DNV
1/8 brace load	saddle	25.43	25.37	25.39	25.41	27.17
	crown	8.20	8.84	8.62	8.41	8.08
1/4 brace load	saddle	25.42	25.32	25.36	25.40	27.17
	crown	8.20	9.49	9.05	8.63	8.08
1/2 brace load	saddle	25.42	25.22	25.30	25.36	27.17
	crown	8.20	10.78	9.91	9.06	8.08

a slight lowering of the SCF due to chord load, but this too is quite insignificant.

At the chord crown position, the effect of chord loading on the SCF show a consistent increase both according to the loading cases, and in comparison with Models I and II. All loading instances show higher SCF than the unloaded case and with highest deviation for the loading instance closest to the crown position. See figures 4.14-4.16. By comparing the SCF values determined for the 1/2 loading case of this model and Model II, it is clear that a higher diameter ratio leads to a higher effect of the chord loading on crown SCF.

Comparing the unloaded FEA case with DNV, it could be observed that SCF from DNV at the chord saddle is conservative even though the gap appeared to be closing off compared to Models I and II. SCF from FEA at crown position show more agreement with results obtained from standard. Even though FEA results are slightly on the conservative side.

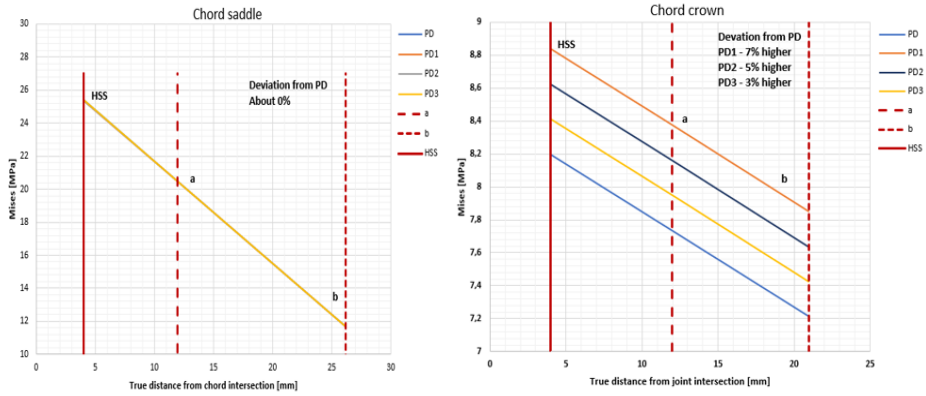


Figure 4.14: Extrapolation of stresses at point a and b to the hot spot for the 1/8 loading case.

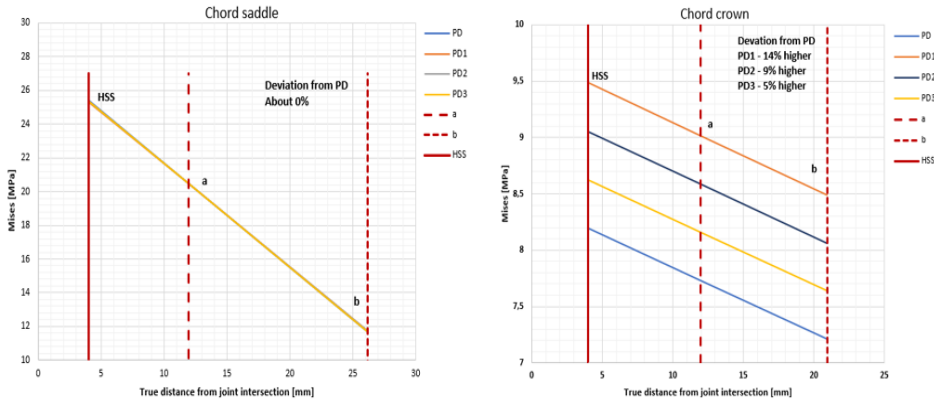


Figure 4.15: Extrapolation of stresses at point a and b to the hot spot for the 1/4 loading case.

4.8 Model IV

The aim of this model is to investigate a Y-joint with a 45 degree inclination angle between the brace and chord. In a Y-joint, axial brace force is reacted by both bending and axial force in the chord as opposed to a T-joint, where axial brace load is reacted by bending in the chord. The T and Y joints are often grouped together as they have similar behaviours. For this model, 2 loading cases were used with 4 loading instances each, 2 on the heel side and 2 of the toe side, giving a total of 8 models. As such, 1/2 and 1/4 represent the loading cases while YT1, YT2 , YH1 and YH2 represent the loading instances. Y is the unloaded case. See figure 4.17. Table 4.9 shows defines the geometry of the Joint used while table 4.10 summarizes the FE model.

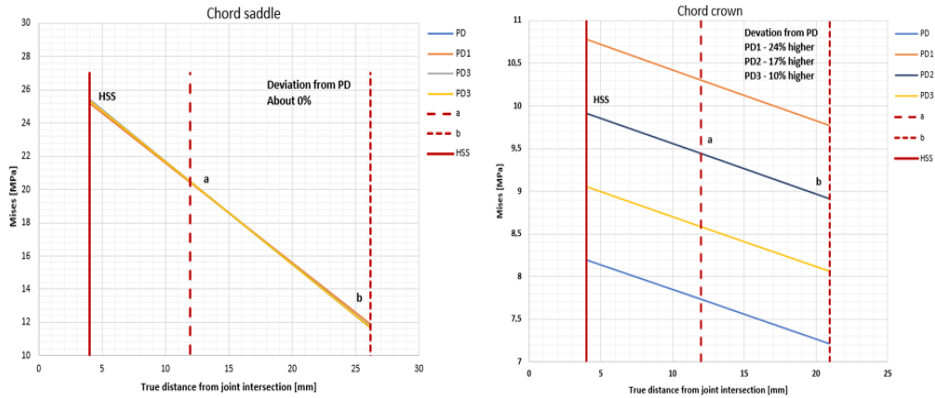


Figure 4.16: Extrapolation of stresses at point a and b to the hot spot for the 1/2 loading case.

Table 4.9: Definition of joint geometry.

Parameter	Chord	Brace
Length	3302 mm	-
Outer diameter	508 mm	243.84 mm
Thickness	15.97 mm	10.06 mm

Table 4.10: Summary of Model IV

Tubular Y-joint with long chord, $\alpha > 12$	
Element type	Shell, S8R
Method for read out of stress	a and b
Weld toe location	Assumed as 0.5t
Axial brace load	7319.4 N
Number of nodes around circumference	106
Nodal loads applied for 1/4, 1/2 loading cases	17.43 N, 34.87 N
Distances of chord load from crown position	See figure 4.17

4.8.1 Results and observations

SCFs were determined for each loading instance for all loading cases and the results are shown in table 4.11. Results are plotted for better visualization as shown by figures 4.19-4.20. Hot spot stresses on these plots also represent SCFs. Figure 4.18 shows contour plots of Mises stresses for averaged and unaveraged results with very slight deviation between the two, yet indicating a well converged mesh. The averaged results were used to compute

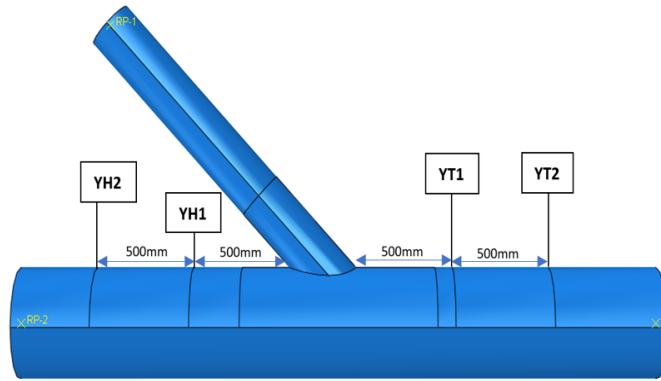


Figure 4.17: Illustration of partition lines for application of chord load for the Y-joint.

SCFs.

At the chord saddle position, chord loading does not show any effect on the SCFs. It does not seem to matter where the chord load is applied, be it the heel or the toe side of the brace. This is similar to what is observed in Models I,II and III.

At the chord crown position, the effect of chord loading is quite visible, showing an increase in SCF on both toe and heel side loading. Also as observed in the T-joint, the closer the load to the brace, the higher the effect of chord loading. However chord loading for the same loading case showed higher SCF on the toe side than on the heel side. This is likely because SCFs were determined from stresses extracted at the toe side of the brace.

Comparing the unloaded Y case and DNV, results show the same pattern as observed in Models I and II. Whereby DNV results at the chord saddle tend to be conservative, in this case may be a bit too conservative, showing a deviation of about 28 %. while FEA results at the chord crown are on the conservative side, in agreement with [21].

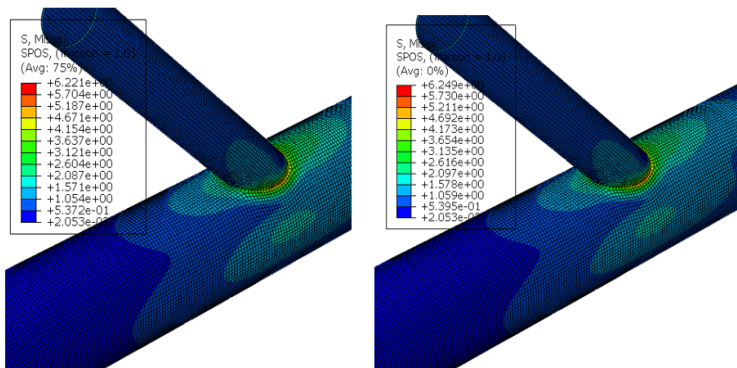


Figure 4.18: Contour plots for Mises stress showing averaged and unaveraged results.

Table 4.11: SCF from FEA Y-joint with loaded chord member.

SCFs for load application at different locations away from the chord crown.							
Load case	position	Y	YH1	YH2	YT1	YT2	DNV
1/4 brace load	saddle	4.51	4.51	4.51	4.50	4.51	6.30
	crown	3.60	3.88	3.73	3.98	3.81	3.39
1/2 brace load	saddle	4.51	4.53	4.51	4.50	4.50	6.30
	crown	3.60	4.16	3.85	4.37	4.01	3.39

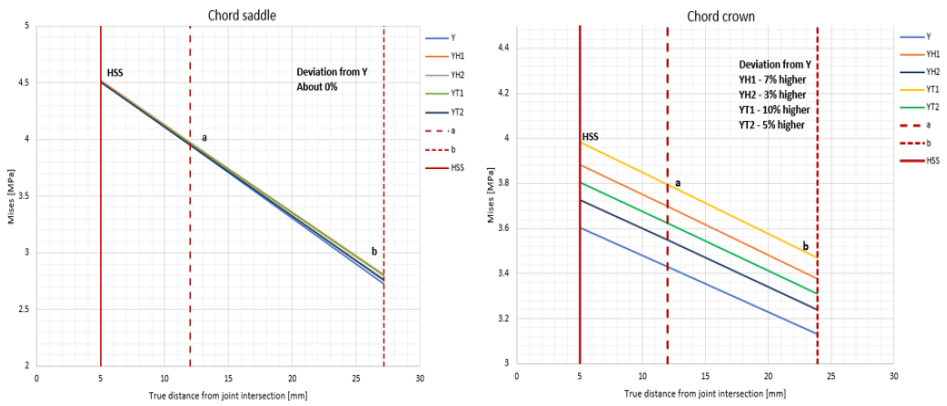


Figure 4.19: Extrapolation of stresses at point a and b to the hot spot for the 1/4 loading case.

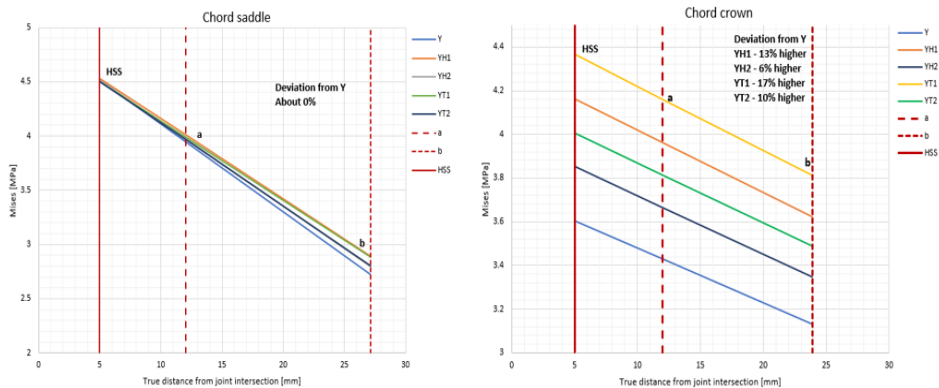


Figure 4.20: Extrapolation of stresses at point a and b to the hot spot for the 1/2 loading case.

Conclusion

5.1 Discussion

This section covers an interpretation as well as an explanation of the results of the study. It is also the aim of this section to justify the approach used and to critically evaluate the study as a whole. Some of the key factors for consideration in this regard are discussed below;

5.1.1 Stress concentration using Efthymiou equations

The Efthymiou equations were used in order to quantify/estimate stress concentration for tubular joints investigated in this study, this is as recommended by industry standards such as DNV-RP-C203 and ISO-19902. The Efthymiou equations are quite popular and cover SCFs in the more common joint types under all relevant brace force conditions. The expressions were based on extensive FEA using thick shell elements for modelling chord and braces, and weld modelling using 3-D brick elements. The key attribute of the Efthymiou equations is that they are quite robust, in that they are found to provide a good fit to the screened SCF database from steel joint tests with a bias of about 10% to 25% on the conservative side [9]. This level of fit and coverage of more joint types than most other SCF equations made them a natural choice for use by designers in the industry. Their usage makes designs more convenient as the bias allows for the incorporation of safety factors into design.

However, as discussed in this report, loaded chord members as defined in the context of this study are not covered by the Efthymiou equations even though such loading is common practice. Therefore with regards to tubular joints with loaded chord members, results from the Efthymiou equations were only used as a point of reference.

Loading condition is the key difference between the Efthymiou equations used and FEM in this study. The former used axial brace load, while the latter used axial brace load in addition to distributed vertical circumferential load on the chord. This difference deems a

direct comparison between results from the two procedures risky. Therefore comparisons are considered to be more appropriate between results from Efthymiou equations and results from the unloaded cases. On that regard, FEA and the Efthymiou equations yielded results that showed fair agreement, with deviations being mainly within the 25% bias.

5.1.2 Stress concentration using FEA

FEA results were determined following as diligently as possible, recommendations from DNV-RP-C203. This is with regards to choice of element formulation, mesh density around hot spot areas as well as derivation of hot spot stresses for determination of SCFs. Hot spot stresses were mainly derived by linear extrapolation of stresses obtained from analysis at distances a and b from the weld toe. This procedure is described under section 4.2 in DNV-RP-C203. While the averaged Von Mises stress was used for calculation of SCFs. The maximum absolute Von Mises stresses were also found to give about the same results. Determination of stress concentration was mainly focused on the chord members since additional loading is not expected to have an effect on brace SCFs [10].

With regards to FEA results for loaded versus unloaded cases, loaded cases demonstrated a noticeable deviation from unloaded cases, with the effects of chord loading mainly manifesting in the crown SCF. Higher deviations were recorded for loads applied closest to the chord crown, and deviations were generally observed to be dependent on the behaviour of the joint under investigation. No observable effect was noticed on the saddle SCFs for all the models investigated. These findings agree with what is obtainable in ISO-19902 [9] and what was found by [10] regarding chord loading. They pointed out that chord bending, -which could result from chord loading as defined in this project- primarily influences crown SCFs. This has been discussed in section 4.2 of the report.

The highest deviation recorded between a loaded and unloaded case was about 24%, which is for the 1/2 loading case and PD1 loading instance of Model III. This brings to question whether or not the Efthymiou equations can be used for design purposes involving joints with loaded chord members as defined in this project. This is a very difficult question to answer. Looking at the just mentioned case, the 24% deviation almost equals the bias that makes results from the Efthymiou equations conservative as compared to steel joints tests or FEA as in this project. This is just a single loading case with a certain magnitude of load at a defined distance away from the crown. It is also a point of discussion how much load the chord actually gets subjected to in practice. This is another difficult question to answer due to the complex nature of loads in jacket structures. But for the sake of perspective, the case in question assumed half the magnitude of the brace load as the load acting on the chord.

5.1.3 Factors influencing the effect of chord loading

Some of the factors that were found to influence the effect of chord loading are discussed under this section;

- **Chord length** : The chord length was found to influence the effect of chord loading. This is easily seen by comparing results of loaded cases from Models I and II, With all other geometric parameters been equal for the two models except the chord length parameter α , Model II showed a much higher deviation between loaded and unloaded cases for the same magnitude of loads on the chord. With a highest deviation of 7% and 16% for the 1/2 loading cases of models I and II respectively. This is a manifestation of the problem that the short chord correction factors in relation to the Efthymiou equations are meant to address in joints with $\alpha < 12$.
- **Diameter ratio**: The ratio of the brace diameter to the chord diameter is found to influence the effect of chord loading. This is seen by comparing the 1/2 loading case of Model II and 1/4 of Model III. It can be observed that, for higher magnitude of chord load, Model III showed a lower deviation (about 14 %) between loaded and unloaded cases due to a higher diameter ratio, compared to the 16 % showed by Model II with a lower magnitude of load and a lower diameter ratio. So the higher the diameter ratio, the lower the effect of chord loading.
- **Distance of chord load from crown position** : The distance of chord load from crown position has been found to influence the effect of chord loading, this was observed consistently in all the models investigated. And as it turned, the closer the chord load to the crown position, the higher the deviation expected between loaded and unloaded case.
- **Type of joint**: Although most of the joints investigated under this study are simple T-joints, the only Y-joint investigated seemed to show quite some similarities but also some differences to the behaviour of T-joints under chord loading. The main source of difference is which side of the brace chord load is applied. Overall, chord loads applied on the toe side of the brace appeared to show higher deviations from unloaded cases.

5.2 Conclusion

The aim of this study was to carry out stress analysis of simple tubular joints using the finite element method as well as industry standard DNV-RP-C203. Focus was mainly to be on estimating stress concentration factors for joints with loaded chord members. A total of 35 models were run, subject to different magnitudes of loading and at different distances away from the chord crown, the results were computed analyzed and discussed, It is on that basis that the following conclusive remarks will be made;

- At chord crown positions, chord loading as defined in this thesis was found to have an effect of increasing SCFs. An increase as high as 24% was recorded between loaded and unloaded cases. This result agreed with what was found in the literature.
- At chord saddle positions, chord loading as defined in the thesis was found to have no observable effect on the SCFs. This is true for all the joints studied. This finding is also in agreement with what is available in the literature.
- Factors such as the chord length parameter, the brace/chord diameter ratio were found to have an influence on the effect generated from chord loading. Other factors include the distance of chord load from the crown position as well as the type of joint under investigation.
- However, in order to provide a definite solution to stress concentration problems of tubular joints with loaded chord members, more holistic investigations need to be carried out, a part of which could be the recommendations in section 5.3.

5.3 Further work

Although a considerable amount of work has been done to investigate the effect of chord loading on stress concentration in this study, It is the opinion of the author that a lot more needs to be done in order to adequately address the problem, to the point of, say, providing generalized equations/solutions that can be used for design purposes involving tubular joints with loaded chord members. To that end, the author has the following recommendations;

- There should be an extensive coverage of the more common types of joints used in jacket structures especially the K and KT joints. These are very common joint types and their coverage will allow a better understanding of the effects of chord loading as discussed in this project.
- There should be a more thorough exploration of the options provided by FEA especially in terms of element formulation. Solid element modelling should certainly be considered allowing modelling of welds and thus better capturing of geometric stresses.
- Even though this can be expensive, physical experiments can provide a better point of reference for FEA. This would provide a lot of observational data which can aid understanding of the behaviours of joints under such loading.
- Collaboration with industry can also bring a lot of perspective into an investigation like this. This would mainly provide an idea on the magnitude chord loading obtainable in practice.

Bibliography

- [1] Abaqus/cae user's manual.
- [2] Hamid Ahmadi and Ali Ziaei Nejad. Geometrical effects on the local joint flexibility of two-planar tubular dk-joints in jacket substructure of offshore wind turbines under opb loading. *Thin-Walled Structures*, 114:122–133, 05 2017.
- [3] E Chang and WD Dover. Prediction of stress distributions along the intersection of tubular y and t-joints. *International Journal of Fatigue*, 21(4):361–381, 1999.
- [4] Kok-Hon Chew, K. Tai, Eddie Ng, and Michael Muskulus. Analytical gradient-based optimization of offshore wind turbine substructures under fatigue and extreme loads. *Marine Structures*, 47:23–41, 05 2016.
- [5] YS Choo, XD Qian, and J Wardenier. Effects of boundary conditions and chord stresses on static strength of thick-walled chs k-joints. *Journal of Constructional Steel Research*, 62(4):316–328, 2006.
- [6] Value design consulting. Investigating fea results.
- [7] DNVG DNVGL-RP. C203: Fatigue design of offshore steel structures. *Det Norske Veritas AS, Oslo, Norway*, 2014.
- [8] Petros Dratsas. Prediction of fatigue crack growth behaviour of tubular joints used in offshore structures. 2016.
- [9] BS EN ISO. 19902: Petroleum and natural gas industries — fixed steel offshore structures. *British standards*, 2013.
- [10] Spyros A Karamanos, Arie Romeijn, and Jaap Wardenier. Scf equations in multi-planar welded tubular dt-joints including bending effects. *Marine structures*, 15(2):157–173, 2002.
- [11] Anders Kleven. Evaluation of scfs for stiffened tubular joints. Master's thesis, University of Stavanger, Norway, 2015.

-
- [12] MMK Lee. Strength, stress and fracture analyses of offshore tubular joints using finite elements. *Journal of Constructional Steel Research*, 51(3):265–286, 1999.
- [13] Hirpa G. Lemu. Stress life diagram, (s-n diagram).
- [14] Jeron Maheswaran. Fatigue life estimation of tubular joints in offshore jacket according to the scfs in dnv-rp-c203, with comparison of the scfs in abaqus/cae. Master's thesis, University of Stavanger, Norway, 2014.
- [15] R W Nicholson. Linear and non-linear analysis - options and advantages for tubular joint design. In *Design of tubular joints for offshore structures: a UEG conference to discuss developments and the impact of a new and rational approach*, London, England, 1985.
- [16] ABS Plaza. Fatigue assessment of offshore structures. 2003.
- [17] AB Potvin, JG Kuang, RD Leick, JL Kahlich, et al. Stress concentration in tubular joints. *Society of Petroleum Engineers Journal*, 17(04):287–299, 1977.
- [18] Lloyd's register of shipping. *Stress concentration factors for simple tubular joints*. Health and safety executive, 1997.
- [19] Ed Sieveka. Concepts and applications of finite element analysis: by robert d. cook, wiley, new york, isbn 0-471-03050-3, 1981, 537 pages, 1985.
- [20] Dr. I E Tebbett. Design substantiation through physical model testing. In *Design of tubular joints for offshore structures: a UEG conference to discuss developments and the impact of a new and rational approach*, London, England, 1985.
- [21] Philippe Thibaux and Steven Cooreman. Computation of stress concentration factors for tubular joints. In *International Conference on Offshore Mechanics and Arctic Engineering*, volume 55331, page V02BT02A011. American Society of Mechanical Engineers, 2013.
- [22] II UEG. Design of tubular joints for offshore structures. *UEG Publication UR33, UEG/CIRIA*, 1985.
- [23] Ke Wang, Le-Wei Tong, Jun Zhu, Xiao-Ling Zhao, and Fidelis R Mashiri. Fatigue behavior of welded t-joints with a chs brace and cfchs chord under axial loading in the brace. *Journal of Bridge Engineering*, 18(2):142–152, 2013.
- [24] J Wardenier, Y Kurobane, JA vd Packer, GJ Van der Vegte, and XL Zhao. Design guide 1 for circular hollow section (chs) joint under predominantly static loading, 2nd. *CIDECT, Construction with hollow steel sections*, 2008.
- [25] John Wægter. Stress concentrations in simple tubular joints. 2009. 3.1.

Appendix

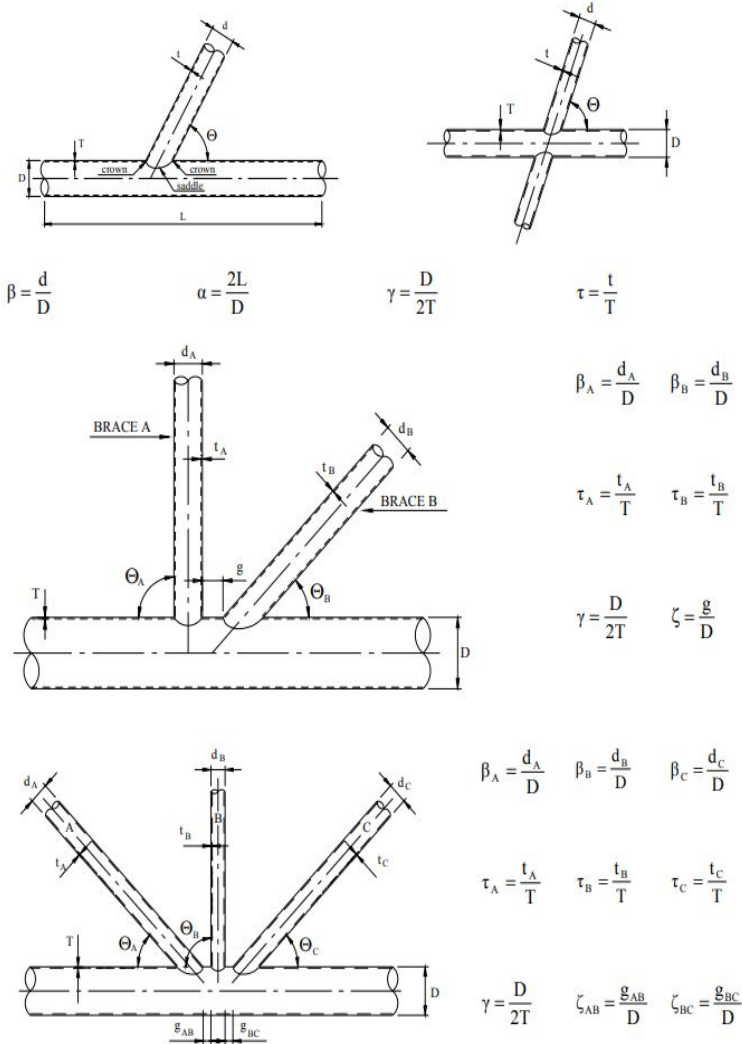


Figure B-2 Definition of geometrical parameters.

The validity range for the equations in Table B-1 to Table B-5 is as follows:

$$\begin{aligned}
 0.2 &\leq \beta \leq 1.0 \\
 0.2 &\leq \tau \leq 1.0 \\
 8 &\leq \gamma \leq 32 \\
 4 &\leq \alpha \leq 40 \\
 20^\circ &\leq \theta \leq 90^\circ \\
 \frac{-0.6\beta}{\sin\theta} &\leq \zeta \leq 1.0
 \end{aligned}$$

Reference is made to Section [4.2] if actual geometry is outside validity range.

Table B-1 Stress concentration factors for simple tubular T/Y joints

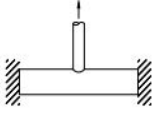
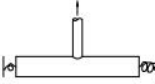
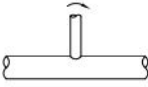
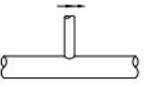
Load type and fixity conditions	SCF equations	Eqn. No.	Short chord correction	
Axial load- Chord ends fixed 	Chord saddle: $\gamma \tau^{1.1} (1.11 - 3(\beta - 0.52)^2) (\sin \theta)^{1.6}$	(1)	F1	
	Chord crown: $\gamma^{0.2} \tau (2.65 + 5(\beta - 0.65)^2) + \tau \beta (0.25\alpha - 3) \sin \theta$	(2)	None	
	Brace saddle: $1.3 + \gamma \tau^{0.52} \alpha^{0.1} (0.187 - 1.25\beta^{1.1}(\beta - 0.96)) (\sin \theta)^{(2.7-0.01\alpha)}$	(3)	F1	
	Brace crown: $3 + \gamma^{1.2} (0.12 \exp(-4\beta) + 0.011\beta^2 - 0.045) + \beta \tau (0.1\alpha - 1.2)$	(4)	None	
Axial load- General fixity conditions 	Chord saddle: (Eqn.(1)) + $C_1(0.8\alpha - 6)\tau\beta^2(1 - \beta^2)^{0.5}(\sin 2\theta)^2$	(5)	F2	
	Chord crown: $\gamma^{0.2} \tau (2.65 + 5(\beta - 0.65)^2) + \tau \beta (C_2\alpha - 3) \sin \theta$	(6a)	None	
	Alternatively $SCF_{c_c} = \gamma^{0.2} \tau (2.65 + 5(\beta - 0.65)^2) - 3\tau \beta \sin \theta + \frac{\sigma_{BendingChord}}{\sigma_{Axialbrace}} SCF_{att}$	(6b)		
	where $\sigma_{BendingChord}$ = nominal bending stress in the chord $\sigma_{Axialbrace}$ = nominal axial stress in the brace. SCF_{att} = stress concentration factor for an attachment = 1.27			
	Brace saddle: (Eqn. (3))		F2	
	Brace crown: $3 + \gamma^{1.2} (0.12 \exp(-4\beta) + 0.011\beta^2 - 0.045) + \beta \tau (C_3\alpha - 1.2)$	(7a)	None	
	Alternatively $SCF_{c_c} = 3 + \gamma^{1.2} (0.12 \exp(-4\beta) + 0.011\beta^2 - 0.045) - 1.2\beta\tau + \frac{0.4\sigma_{BendingChord}}{\sigma_{Axialbrace}} SCF_{att}$	(7b)		

Table B-1 Stress concentration factors for simple tubular T/Y joints (Continued)

In-plane bending 	Chord crown:	(8)	None
	$1.45\beta \tau^{0.85} \gamma^{(1-0.68\beta)} (\sin \theta)^{0.7}$ Brace crown: $1 + 0.65\beta \tau^{0.4} \gamma^{(1.09-0.77\beta)} (\sin \theta)^{(0.06\gamma-1.16)}$	(9)	None
Out-of-plane bending 	Chord saddle:	(10)	F3
	$\gamma \tau \beta (1.7 - 1.05\beta^3) (\sin \theta)^{1.6}$ Brace saddle: $\tau^{-0.54} \gamma^{-0.05} (0.99 - 0.47\beta + 0.08\beta^4)$ (Eqn. 10)	(11)	F3
Short chord correction factors ($\alpha < 12$) $F1 = 1 - (0.83\beta - 0.56\beta^2 - 0.02) \gamma^{0.23} \exp(-0.21 \gamma^{-1.16} \alpha^{2.5})$ $F2 = 1 - (1.43\beta - 0.97\beta^2 - 0.03) \gamma^{0.04} \exp(-0.71 \gamma^{-1.38} \alpha^{2.5})$ $F3 = 1 - 0.55 \beta^{1.8} \gamma^{0.16} \exp(-0.49 \gamma^{-0.89} \alpha^{1.8})$ where $\exp(x) = e^x$		Chord-end fixity parameter $C1 = 2(C-0.5)$ $C2 = C/2$ $C3 = C/5$ $C =$ chord end fixity parameter $0.5 \leq C \leq 1.0$, Typically $C = 0.7$	

It should be noted that equations (6b) and (7b) will for general load conditions and moments in the chord member provide correct hot spot stresses at the crown points while equations (6a) and (7a) only provides correct hot spot stress due to a single action load in the considered brace. Equations (6b) and (7b) are also more general in that a chord-fixation parameter need not be defined. In principle it can account for joint flexibility at the joints when these are included in the structural analysis. Also the upper limit for the α -parameter is removed with respect to validity of the SCF equations. Thus, these equations are in general recommended used.

Equation (6a) and (6b) will provide the same result only for the special case with a single action load in the considered brace and $SCF_{att} = 1.0$. For long chords the brace can be considered as an attachment to the chord with respect to axial stress at the crown points. This would give detail category F from Table A-7 (for thick braces and E-curve for thinner) which corresponds to $SCF_{att} = 1.27$ from Table 2-1.